Supplementary Information

Synthesis and photoluminescent properties of polynorbornenes bearing platinum complex and diphenylanthracene moieties in the side chains

Yuki Horino,[a] Ryota Kobayashi,[a] Toshiko Mizokuro,[b] Hiromitsu Sogawa,[a] Fumio Sanda*,[a]

[a] Department of Chemistry and Materials Engineering, Faculty of Chemistry, Materials and Bioengineering, Kansai University, 3-3-35 Yamate-Cho, Suita, Osaka 564-8680, Japan

[b] National Institute of Advanced Industrial Science and Technology (AIST), 1-1-1 Higashi, Tsukuba, Ibaraki 305-8565, Japan

* Corresponding author.

E-mail: sanda@kansai-u.ac.jp (F. Sanda)

Experimental

Reagents

Bis(triphenylphosphine)palladium(II) dichloride $[PdCl_2(PPh_3)_2]$,[S1] tetrakis(triphenylphosphine)palladium(0) $[Pd(PPh_3)_4]$,[S2] [1,1'-bis(diphenylphosphino)ferrocene]palladium(II) $[Pd(dppf)Cl_2]$[S3] and dichloro[1,3-bis(2,4,6-trimethylphenyl)-2-imidazolidinylidene]-(benzylidene)bis(3-bromopyridine)ruthenium(II) (Grubbs 3rd generation catalyst) (**G3**),[S4] were synthesized according to the literature. $PtI_2(PEt_3)_2$ was synthesized from potassium tetrachloroplatinate(II) (K_2PtCl_4), PEt_3 and KI according to a literature method.[S5] 4-Bromobenzylamine hydrochloride (Tokyo Chemical Industry Co., Ltd.), *cis*-5-norbornene-exo-2,3-dicarboxylic anhydride (BLD Pharmatech Ltd.), NaOH (Kanto Chemical Co., Inc.), triphenylphosphine (FUJIFILM Wako Pure Chemical Co.), CuI (NACALAI TESQUE, INC.), trimethylsilylacetylene (TMSA) (Apollo Scientific Ltd.), 4-bromo-1,8-naphthalic anhydride (Tokyo Chemical Industry Co., Ltd.), hexylamine (Sigma-Aldrich), tetrabutylammonium fluoride (TBAF, *ca*. 1 mol/L in THF) (Tokyo Chemical Industry Co., Ltd.), K_2PtCl_4 (FUJIFILM Wako Pure Chemical Co.), 9-bromoanthracene (Tokyo Chemical Industry Co., Ltd.), 9-phenylanthracene (Angene International Limited), phenylboronic acid (FUJIFILM Wako Pure Chemical Co.), *N*-bromosuccinimide (NBS) (FUJIFILM Wako Pure Chemical Co.), bis(pinacolato)diboron (BLD Pharmatech Ltd.), ethyl vinyl ether (Tokyo Chemical Industry Co., Ltd.), potassium carbonate (NACALAI TESQUE,

INC.), potassium acetate (Sigma-Aldrich), NaCl (FUJIFILM Wako Pure Chemical Co.), HCl (35%) (NACALAI TESQUE, INC.), $MgSO_4$ (FUJIFILM Wako Pure Chemical Co.), toluene (NACALAI TESQUE, INC.), dichloromethane (NACALAI TESQUE, INC.), chloroform (NACALAI TESQUE, INC.), ethyl acetate (NACALAI TESQUE, INC.), hexane (NACALAI TESQUE, INC.), acetic acid (NACALAI TESQUE, INC.), ethanol (NACALAI TESQUE, INC.), diethyl ether (NACALAI TESQUE, INC.), triethylamine (NACALAI TESQUE, INC.), DMF (NACALAI TESQUE, INC.), THF (NACALAI TESQUE, INC.), DMSO (NACALAI TESQUE, INC.), acetone (NACALAI TESQUE, INC.), EtOH (NACALAI TESQUE, INC.), 1,4-dioxane (NACALAI TESQUE, INC.) were used without purification. Solvents used in reactions under argon or N_2 were dehydrated over molecular sieves 4A 1/16 and degassed by bubbling before use.

Measurements

^{1}H (400 MHz), ^{13}C (100 MHz), and ^{31}P (162 MHz) NMR spectra were measured on a JEOL JNM-ECS400 spectrometer and a JEOL JNM-ECZ400 spectrometer. Melting point (mp) was measured using a Yanaco micro melting point apparatus. IR absorption spectra were measured on a JASCO FTIR-4100 spectrophotometer. Mass spectra were acquired with a BRUKER Compact QTOF spectrometer under the following conditions: ionization method, electrospray ionization (ESI); solvent, MeOH; mass range, m/z = 300–2000; mode, positive, calibrated and

tuned using an available standard solution of Low Concentration Tuning mix (Agilent Technologies, G1969-85000). UV–vis absorption spectra were measured on a SHIMADZU UV-2600 spectrophotometer. Photoluminescence (PL) spectra were measured on a SHIMADZU RF-6000 spectrofluorophotometer. Number-average molecular weight (M_n) and dispersity ($Đ$) were determined by a size exclusion chromatography (SEC) system consisting of JASCO RI-4030, UV-4075, PU-4180, DG-980-50, CO-4060, LC-NetII/ADC, AS-2055 Plus, equipped with a Shodex LF-804 polystyrene gel column, calibrated with polystyrene standards.

UC Measurement

Polymers and DPA (if necessary) were dissolved in THF, and stirred in an atmosphere-controlled glove box for at least 60 minutes to remove dissolved oxygen. Each solution was placed in a four-sided transparent quartz optical cell with branches and sealed tightly. The quartz cell was irradiated with a THORLABS CPS450 CW laser (λ = 450 nm, 47 mW/cm^2) through a Chroma Tech. OD6 ZET457NF notch filter (λ = 457 nm). Emission spectra were measured with an Ocean photonics FLAME-S fiber spectrometer. with integration time of 100 ms and number of integrations of 10 times.

Monomer synthesis

Monomers **1** and **2** were synthesized according to Schemes S1–S3.

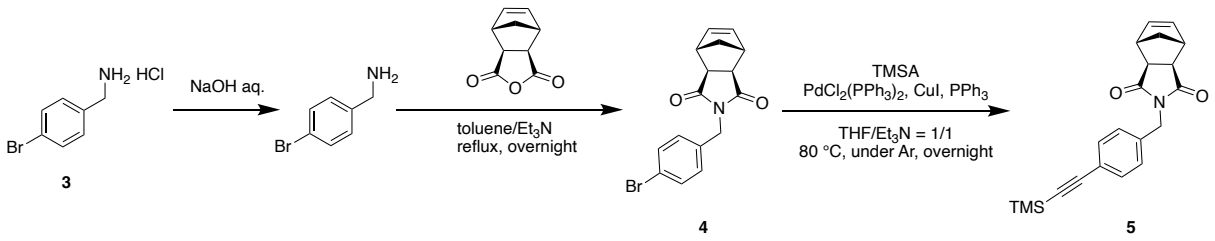

Scheme S1 Synthesis of **5**.

Compound 4

NaOH (0.40 g, 10.0 mmol) was added to a solution of 4-bromobenzylamine hydrochloride (2.23 g, 10.0 mmol) in water (100 mL) until the pH became 12. The solution was extracted with CH_2Cl_2 (50 mL × 3), and the organic layer was dried over anhydrous $MgSO_4$. After filtration, the filtrate was concentrated on an evaporator to obtain 4-bromobenzylamine as a transparent viscous liquid in 94% yield (1.74 g, 9.37 mmol). *cis*-5-Norbornene-*exo*-2,3-dicarboxylic anhydride (1.64 g, 10.0 mmol), toluene (70 mL) and Et_3N (1.39 mL) were added to the 4-bromobenzylamine obtained above, and the resulting mixture was stirred at 120 °C overnight. The mixture was cooled to room temperature, and subsequently washed with toluene (50 mL), 0.1 M HCl aq. (50 mL × 3), saturated sodium chloride aq. (50 mL × 3). Recrystallization with a mixture of ethyl acetate and hexane to obtain **4** as a white solid in 97% yield (1.80 g, 9.67 mmol). ^{1}H NMR (400 MHz, $CDCl_3$): δ 1.02 (d, J = 10.1 Hz, –CHCH_2–, 1H), 1.42 (dt, J = 9.9, 1.5 Hz, –CHCH_2–, 1H), 2.68 (d, J = 0.9 Hz, –CH_2CH–, 2H), 3.25 (t, J = 1.8 Hz, –CH–, 2H), 4.56 (s, –CH_2–, 2H), 6.28 (t, J = 1.6 Hz, –CH=CH–, 2H), 7.25–7.28 (m, Ar, 2H), 7.43 (dt, J =

8.7, 2.2 Hz, Ar, 2H) ppm (Fig. S1).

Compound 5

Compound **4** (1.66 g, 5.00 mmol), $PdCl_2(PPh_3)_2$ (35.1 mg, 5.00×10^{-2} mmol), CuI (9.52 mg, 5.00×10^{-2} mmol) and PPh_3 (13.1 mg, 5.00×10^{-2} mmol) were dissolved in THF (10 mL) under N_2. Et_3N (10 mL) and TMSA (0.512 mL, 7.50 mmol) were added to the solution, and the resulting mixture was stirred at 80 °C overnight. The reaction mixture was cooled to room temperature, and ethyl acetate (50 mL) was added to the mixture. It was washed with sat. NH_4Cl aq. (200 mL × 3), dried over anhydrous $MgSO_4$, filtered, and the solvent was removed on a rotary evaporator to obtain a white solid. It was purified by silica gel column chromatography eluted with ethyl acetate/hexane = 1/2 (v/v) to obtain **5** as a white solid (1.65 g, 4.73 mmol). Yield: 95%. Mp 154–157 °C. ^{1}H NMR (400 MHz, $CDCl_3$): δ 0.22–0.26 (m, –Si(CH_3)$_3$, 8H), 1.01 (d, J = 9.6 Hz, –CHCH_2–, 1H), 1.40 (d, J = 10.0 Hz, –CHCH_2–, 1H), 2.67–2.71 (m, –CH_2CH–, 2H), 3.23 (d, J = 1.8 Hz, –COCH–, 2H), 4.59 (s, –CH_2–, 2H), 6.27 (t, J = 1.6 Hz, –CH=CH–, 2H), 7.30 (d, J = 8.2 Hz, Ar, 2H), 7.38–7.44 (m, Ar, 2H) ppm (Fig. S2). ^{13}C NMR (100 MHz, $CDCl_3$): δ 0.1, 42.1, 42.6, 45.3, 47.8, 94.7, 104.6, 122.8, 128.8, 132.2, 136.1, 137.9, 177.6 ppm (Fig. S3). IR (KBr): 760, 779, 818, 843, 865, 898, 919, 935, 1146, 1161, 1172, 1223, 1249, 1335, 1355, 1393, 1422, 1494, 1510, 1696, 1771, 2157, 2877, 2900, 2964, 2992, 3013, 3063 cm^{-1} (Fig. S4). ESI-MS (m/z): calcd. 372.1396 ($[C_{21}H_{23}NO_2Si + Na]^+$), found 372.1374

(Fig. S5).

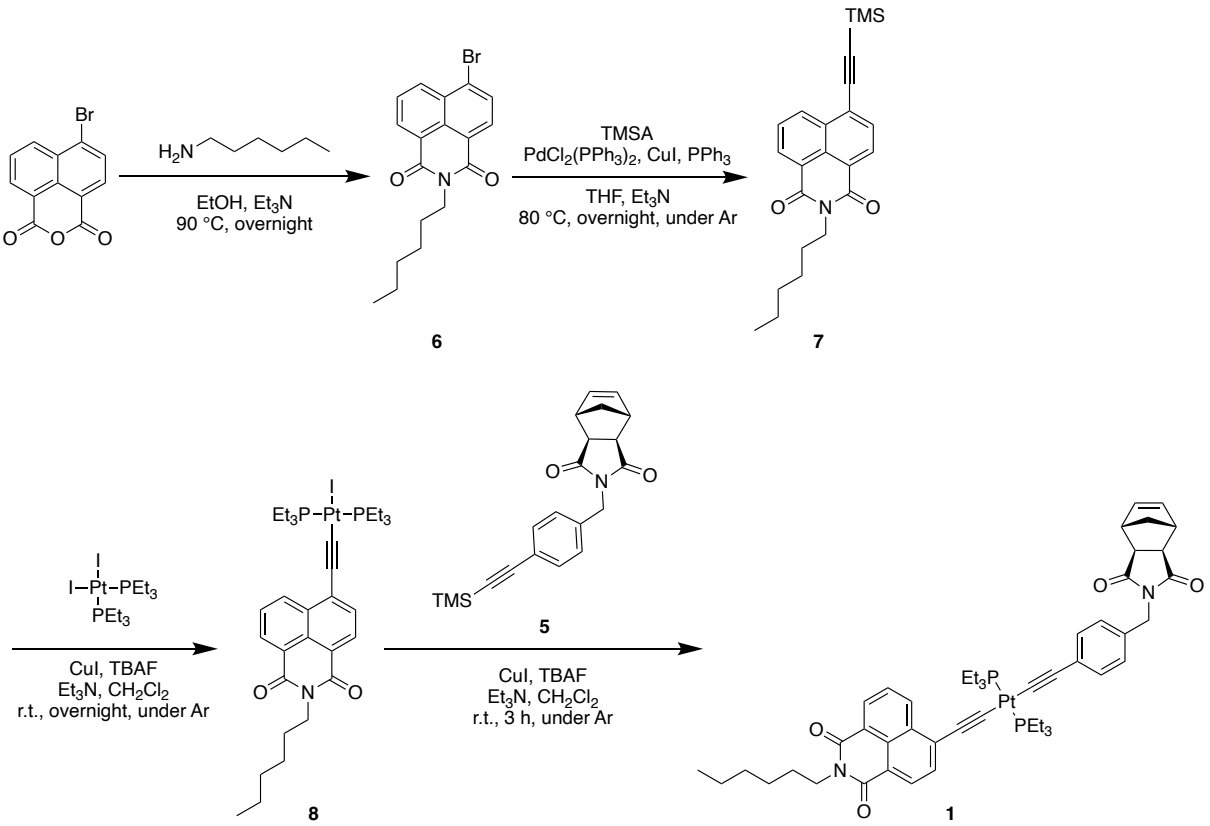

Scheme S2 Synthesis of monomer **1**.

Compound 6

4-Bromo-1,8-naphthlic anhydride (3.32 g, 12.0 mmol) and hexylamine (4.7 mL, 36.0 mmol) were dissolved in EtOH (80 mL). Et_3N (10 mL) were added to the solution, and the resulting mixture was stirred at 80 °C overnight. The reaction mixture was cooled to room temperature. It was purified by silica gel column chromatography eluted with CH_2Cl_2/hexane = 2/1 (v/v) to obtain **6** as a white solid (3.53 g, 9.81 mmol). Yield: 82%. ^1H NMR (400 MHz,

$CDCl_3$): δ 0.87–0.93 (m, $–CH_3$, 3H), 1.25–1.46 (m, $–CH_2–$, 6H), 1.69–1.76 (m, $–CH_2–$, 2H), 4.12–4.20(m, $–CH_2–$, 2H), 7.84 (t, J = 8.6 Hz, Ar, 1H), 8.04 (d, J = 7.8 Hz, Ar, 1H), 8.41 (d, J = 7.5 Hz, Ar, 1H), 8.57 (d, J = 8.4 Hz, Ar, 1H), 8.66 (d, J = 7.2 Hz, Ar, 1H) ppm (Fig. S6).[S6]

Compound 7

Compound **6** (3.53 g, 9.80 mmol), $PdCl_2(PPh_3)_2$ (68.8 mg, 9.8×10^{-2} mmol), CuI (18.7 mg, 9.8×10^{-2} mmol), and PPh_3 (25.7 mg, 9.8×10^{-2} mmol) were dissolved in THF (10 mL) under Ar. Et_3N (10 mL) and TMSA (2.07 mL, 14.7 mmol) were added to the solution, and the resulting mixture was stirred at 80 °C overnight. The reaction mixture was cooled to room temperature, and ethyl acetate (50 mL) was added to the mixture. It was washed with sat. NH_4Cl aq. (200 mL × 3), dried over anhydrous $MgSO_4$, filtered, and the solvent was removed on a rotary evaporator to obtain a brown solid. It was purified by silica gel column chromatography eluted with ethyl acetate/hexane = 1/20 (v/v) to obtain **7** as a white solid (3.19 g, 8.45 mmol). Yield: 86%. ^{1}H NMR (400 MHz, $CDCl_3$): δ 0.35–0.36 (m, $–Si(CH_3)_3$, 9H), 0.89 (t, J = 6.6 Hz, $–CH_3$, 3H), 1.28–1.45 (m, $–CH_2–$, 6H), 1.69–1.79 (m, $–CH_2–$, 2H), 4.17 (t, J = 7.6 Hz, $–CH_2–$, 2H), 7.83 (t, J = 7.8 Hz, Ar, 1H), 7.89 (d, J = 7.8 Hz, Ar, 1H), 8.51 (d, J = 7.3 Hz, Ar, 1H), 8.64 (d, J = 8.0 Hz, Ar, 2H) ppm (Fig. S7). ESI-MS (m/z): calcd. 378.1889 ($[C_{23}H_{27}NO_2Si + H]^+$), found 378.1802 (Fig. S8).

Compound 8

Compound **7** (1.89 g, 5.00 mmol), *cis*-$PtI_2(PEt_3)_2$ (5.14 g, 7.50 mmol), and CuI (14.3 mg, 0.0750 mmol) were dissolved in CH_2Cl_2 (8 mL) under Ar. Et_3N (8 mL) and TBAF (1.0 M in THF) (10.0 mL, 10.0 mmol) were added to the solution, and the resulting mixture was stirred at room temperature overnight. The reaction mixture was cooled to room temperature, and CH_2Cl_2 (50 mL) was added to the mixture. It was washed with sat. NH_4Cl aq. (200 mL × 3), dried over anhydrous $MgSO_4$, filtered, and the solvent was removed on a rotary evaporator to obtain a white solid. It was purified by silica gel column chromatography eluted with CH_2Cl_2/hexane = 1/1 (v/v) to obtain **8** as a yellow solid (2.85 g, 3.30 mmol). Yield: 66%. ^{1}H NMR (400 MHz, $CDCl_3$): δ 0.87–0.94 (m, $–CH_3$, 3H),1.08–1.23 (m, $–CH_3$, 18H), 1.27–1.46 (m, $–CH_2–$, 6H), 1.68–1.76 (m, $–CH_2–$, 2H), 2.15–2.27 (m, $–CH_2–$, 12H), 4.18 (t, J = 7.6 Hz, $–CH_2–$, 2H), 7.65 (d, J = 7.7 Hz, Ar, 1H), 7.72 (t, J = 7.8 Hz, Ar, 1H), 8.46 (d, J = 7.7 Hz, Ar, 1H), 8.59 (dd, J = 7.2, 1.4 Hz, Ar, 1H), 8.72 (dd, J = 8.4, 1.6 Hz, Ar, 1H) ppm (Fig. S9). ^{31}P NMR (160 MHz, $CDCl_3$): δ 9.63 ($J_{Pt–P}$ = 2320 Hz) ppm.

Monomer 1

Compound **8** (1.73 g, 2.00 mmol), compound **5** (0.699 g, 2.00 mmol) and CuI (3.80 mg, 2.00 × 10^{-2} mmol) were dissolved in CH_2Cl_2 (10 mL) under Ar. Et_3N (10 mL) and TBAF (1.0 M in THF) (10.0 mL, 10.0 mmol) were added to the solution, and the resulting mixture was stirred

at room temperature 3 h. The reaction mixture was cooled to room temperature, and CH_2Cl_2 (50 mL) was added to the mixture. It was washed with sat. NH_4Cl aq. (200 mL × 3), dried over anhydrous $MgSO_4$, filtered, and the solvent was removed on a rotary evaporator to obtain a white solid. It was purified by silica gel column chromatography eluted with ethyl acetate /hexane = 1/1 (v/v) to obtain **1** as a yellow solid (1.61 g, 1.59 mmol). Yield: 79%. Mp 60–64 °C. ^{1}H NMR (400 MHz, $CDCl_3$): δ 0.87–0.90 (m, –CH_3, 3H), 1.05–1.11 (m, –CH_2CH–, 1H), 1.19–1.27 (m, –CH_3, 18H), 1.38–1.43 (m, –CH_2CH–, 2H), 1.68–1.76 (m, –CH_2CH_2–, 2H), 2.17 (tt, J = 11.3, 3.8 Hz, –CH_2CH_3, 12H), 2.67 (d, J = 0.9 Hz, –$CHCH_2$–, 2H), 3.25 (t, J = 1.6 Hz, –$CHCH$–, 2H), 4.09–4.18 (m, –CH_2N–, 2H), 4.57 (s, –NCH_2Ph–, 2H), 6.28 (t, J = 1.6 Hz, –CH=CH–, 2H), 7.21–7.26 (m, Ar_2, 4H), 7.62 (d, J = 7.7 Hz, Ar_1, 1H), 7.69 (dd, J = 8.4, 7.5 Hz, Ar_1, 1H), 8.45 (d, J = 7.7 Hz, Ar_1, 1H), 8.57 (dd, J = 7.2, 1.4 Hz, Ar_2, 1H), 8.76 (dd, J = 8.4, 1.1 Hz, Ar_1, 1H) ppm (Fig. S10). ^{13}C NMR (100 MHz, $CDCl_3$): δ 8.3, 14.0, 16.3, 16.5, 16.6, 22.6, 26.8, 28.1, 31.6, 40.3, 42.2, 42.7, 45.3, 47.8, 122.8, 126.0, 128.5, 128.7, 128.8, 131.0, 131.1, 132.1, 132.8, 133.3, 137.9, 164.2, 164.5, 177.7 ppm (Fig. S11). ^{31}P NMR (162 MHz, $CDCl_3$): δ 12.5 ($J_{Pt–P}$ = 2,380 Hz) ppm (Fig. S12). IR (KBr): 615, 640, 662, 717, 732, 757, 768, 782, 853, 890, 930, 1034, 1085, 1145, 1170, 1236, 1348, 1386, 1425, 1456, 1505, 1582, 1657, 1697, 1769, 2085, 2874, 2931, 2961, 3063 cm^{-1} (Fig. S13). ESI-MS (*m*/*z*): calcd. 1012.3911 ($[C_{50}H_{62}N_2O_4P_2Pt + H]^+$), found 1012.3635 (Fig. S14).

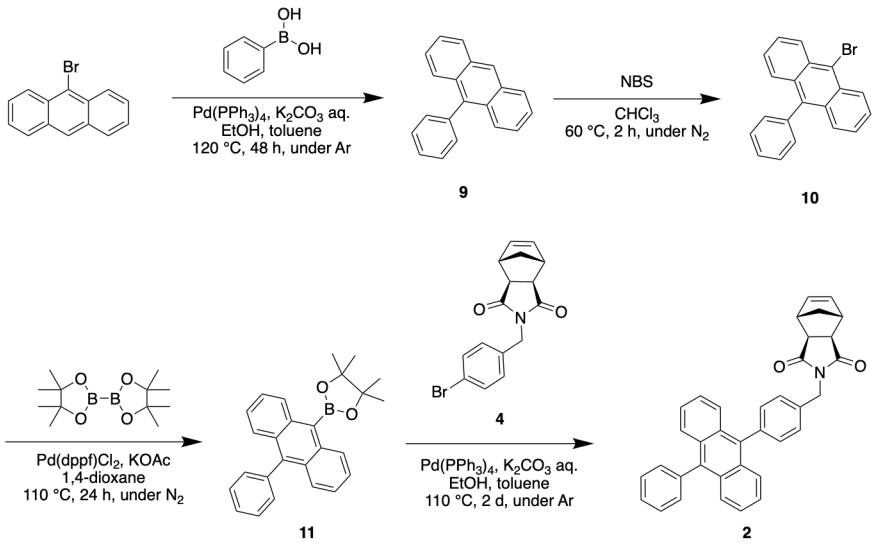

Scheme S3 Synthesis of monomer **3**.[S6]

9-Phenylanthracene (9)

9-Bromoanthracene (1.66 g, 6.46 mmol), phenylboronic acid (1.18 mg, 9.68 mmol) and $Pd(PPh_3)_4$ (74.6 mg, 6.46×10^{-2} mmol) were dissolved in toluene (16 mL) under Ar. K_2CO_3 aq. (2.0 M) (8 mL, 16.0 mmol) and EtOH (4 mL) were added to the solution, and the resulting mixture was stirred at 120 °C for 48 h. The reaction mixture was cooled to room temperature, and CH_2Cl_2 (50 mL) was added to the mixture. It was washed with 0.1 M HCl aq. (200 mL × 3), dried over anhydrous $MgSO_4$, filtered, and the solvent was removed on a rotary evaporator to obtain a white solid. It was purified by silica gel column chromatography eluted with CH_2Cl_2/hexane = 1/2 (v/v) to obtain **9** as a white solid (1.60 g, 6.31 mmol). Yield: 98%.^{1}H NMR (400 MHz, $CDCl_3$): δ 7.25 (s, 1H), 7.32–7.36 (m, 2H), 7.42–7.47 (m, 4H), 7.52–7.60 (m,

3H), 7.65–7.69 (m, 2H), 8.03–8.05 (m, 2H), 8.49 (s, 1H) ppm (Fig. S15).

9-Bromo-10-Phenylanthracene (10)

Compound **9** (1.60 g, 6.31 mmol) and NBS (1.35 g, 7.57 mmol) were dissolved in $CHCl_3$ (80 mL) under Ar, and the resulting mixture was stirred at 60 °C for 2 h. The reaction mixture was cooled to room temperature, and CH_2Cl_2 (50 mL) was added to the mixture. It was washed with pure water (200 mL × 3), dried over anhydrous $MgSO_4$, filtered, and the solvent was removed on a rotary evaporator to obtain **10** as a yellow solid (1.64 g, 4.92 mmol). Yield: 78%. ^{1}H NMR (400 MHz, $CDCl_3$): δ 7.34–7.41 (m, 4H), 7.52–7.66 (m, 7H), 8.58–8.66 (m, 2H) ppm (Fig. S16).

4,4,5,5-Tetramethyl-2-(10-Phenylanthracen-9-yl)-1,3,2-Dioxaborolane (11)

Compound **10** (1.64 g, 4.92 mmol), bis(pinacolato)diboron (1.87 g, 7.38 mmol), Pd(pddf)Cl_2 (0.180 g, 0.246 mmol) and KOAc (2.90 g, 29.5 mmol) were dissolved in 1,4-dioxane (30 mL) under Ar, and the resulting mixture was stirred at 110 °C for 24 h. The reaction mixture was cooled to room temperature, and CH_2Cl_2 (50 mL) was added to the mixture. It was washed with 0.1 M HCl aq. (200 mL × 3), dried over anhydrous $MgSO_4$, filtered, and the solvent was removed on a rotary evaporator to obtain a brown liquid. It was purified by silica gel column chromatography eluted with CH_2Cl_2/hexane = 1/1 (v/v) to obtain **11** as a white solid (1.21 g, 3.19 mmol). Yield: 65%. ^{1}H NMR (400 MHz, $CDCl_3$): δ 1.58–1.65 (m, –CH_3, 12H), 7.29–7.63

(m, Ar, 11H), 8.43 (d, J = 8.6 Hz, Ar, 2H) ppm (Fig. S17).

Monomer 2

Compound **11** (1.64 g, 4.31 mmol), compound **4** (1.15 g, 3.45 mmol) and $Pd(PPh_3)_4$ (200 mg, 0.17 mmol) were dissolved in toluene (20 mL) under Ar. EtOH (4 mL) and 3.0 M K_2CO_3 aq. (4.3 mL, 12.9 mmol) were added to the solution, and the resulting mixture was stirred at 110 °C for 2 days. The reaction mixture was cooled to room temperature, and CH_2Cl_2 (50 mL) was added to the mixture. It was washed with 0.1 M HCl aq. (200 mL × 3), dried over anhydrous $MgSO_4$, filtered, and the solvent was removed on a rotary evaporator to obtain a brown liquid. It was purified by silica gel column chromatography eluted with $CHCl_3$ to obtain **2** as a yellow solid (1.54 g, 3.05 mmol). Yield: 89%. Mp 246–250 °C. ^{1}H NMR (400 MHz, $CDCl_3$): δ 1.22–1.26 (m, –CHCH_2–, 1H), 1.52 (d, J = 10.0 Hz, –CHCH_2–, 1H), 2.79 (d, J = 0.9 Hz, –CHCH–, 2H), 3.35 (s, –COCH–, 2H), 4.82 (s, –NCH_2–, 2H), 6.33 (d, J = 1.8 Hz, –CH=CH–, 2H), 7.29–7.33 (m, Ar, 4H), 7.42–7.48 (m, 4H), 7.52–7.70 (m, Ar, 9H) ppm (Fig. S18). ^{13}C NMR (100 MHz, $CDCl_3$): δ 42.4, 42.8, 45.5, 48.1, 125.1, 126.9, 127.1, 127.6, 128.5, 128.9, 129.9, 131.4, 131.8, 135.2, 136.6, 137.3, 138.1,138.8, 139.1, 178.0 ppm (Fig. S19). IR (KBr): 893, 942, 1021, 1108, 1151, 1176, 1303, 1348, 1366, 1389, 1413, 1427, 1442, 1514, 1706, 1770, 2874, 2978, 3060 cm^{-1} (Fig. S20). ESI-MS (m/z): calcd. 506.2120 ($[C_{36}H_{27}NO_2 + H]^+$), found 506.2107 (Fig. S21).

Polymerization

The copolymerizations of **1** and **2** were performed as shown in Scheme S4. The typical procedure is as follows.

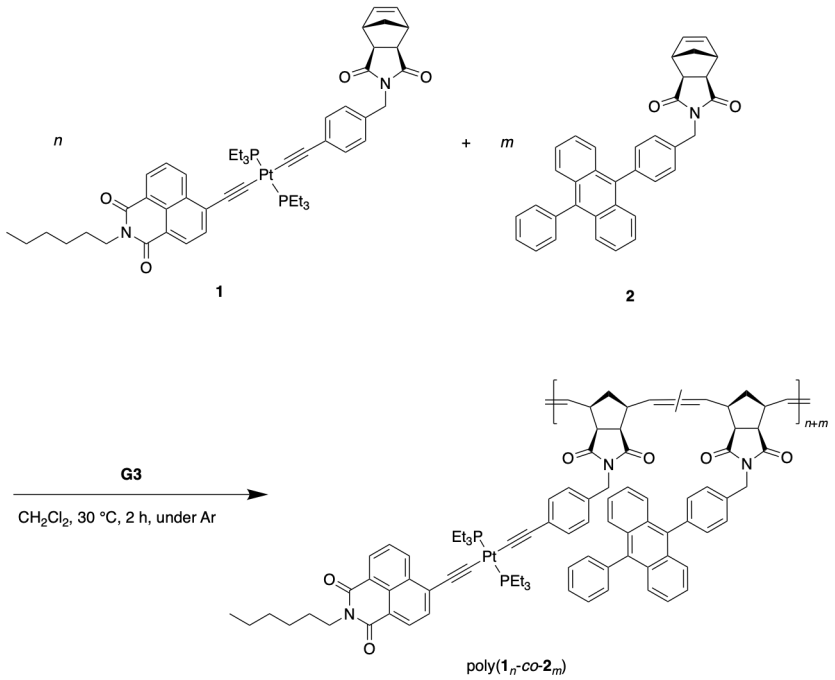

Scheme S4 Synthesis of poly(**1**$_n$-*co*-**2**$_m$).

Monomer **1** (121.5 mg, 0.12 mmol) and **2** (60.67 mg, 0.12 mmol) were dissolved in CH_2Cl_2 (1.9 mL) under Ar. A CH_2Cl_2 solution (0.5 mL) of **G3** (2.12 mg, 0.0024 mmol) were added to the solution, and the resulting mixture was stirred at 30 °C for 2 h. Ethyl vinyl ether (1.2 mL, 0.012 mmol) was added and the reaction mixture, and the resulting mixture was stirred for 30 minutes. The reaction mixture was poured into MeOH (200 mL), and the mixture was stirred

for 1 hour to precipitate a solid mass. It was collected using a membrane filter (pore size = 1.0 μm) and dried to obtain poly(**1**$_{50}$-*co*-**2**$_{50}$) as a yellow film-like solid (134 mg, yield: 74%) The ^{1}H and ^{31}P NMR spectra of the poly(**1**$_{50}$-*co*-**2**$_{50}$) are shown in Figs. S22 and S23, and those of poly(**1**$_{20}$-*co*-**2**$_{100}$) and poly(**1**$_{10}$-*co*-**2**$_{100}$) are shown in Figs. S24–S27.

Computation

All computational calculations were performed with the Gaussian 16,[S7] Fujitsu-Arm-G16 Rev C.01, using the DFT method with B3LYP functional in conjunction with basis sets, 6-31G* for H, C, N, O, P and LANL2DZ for Pt, running on the supercomputer system, Fugaku provided by the RIKEN Center for Computational Science. The UV–vis absorption, fluorescence and phosphorescence spectra were simulated by the TD-DFT method, and plotted with a peak half-width height = 0.2 eV using GaussView 6.

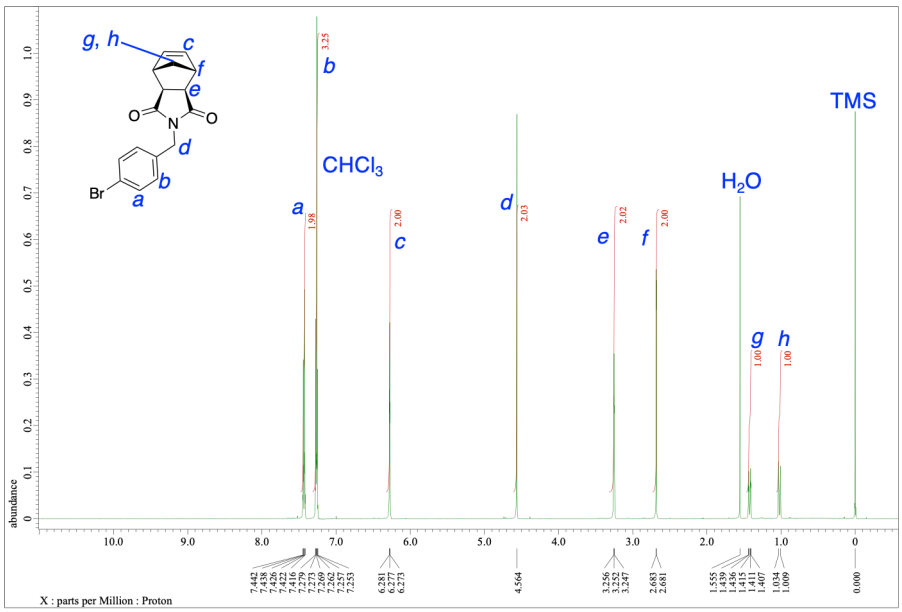

Fig. S1 ^{1}H NMR (400 MHz) spectrum of **4** measured in $CDCl_3$.

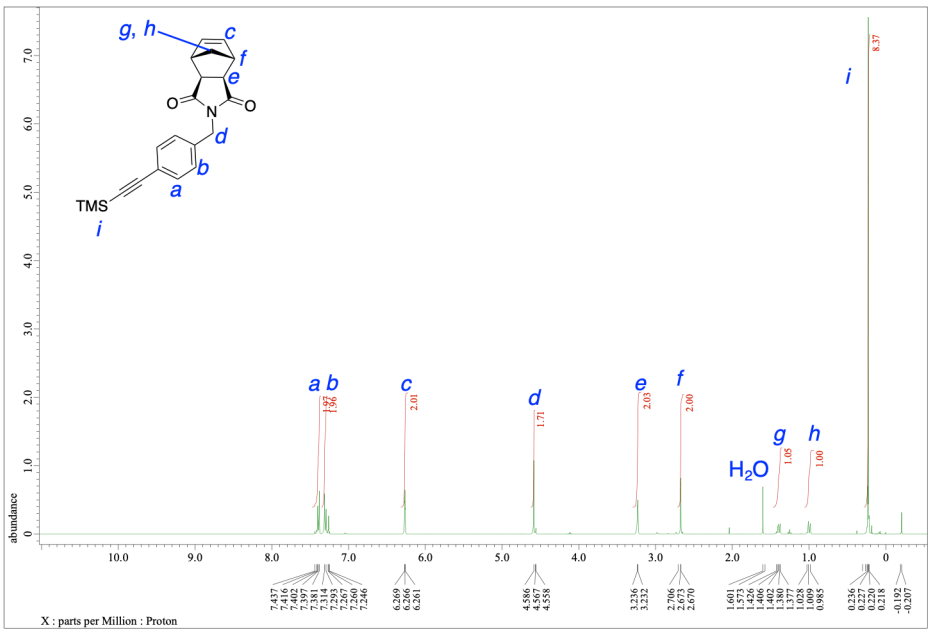

Fig. S2 ^{1}H NMR (400 MHz) spectrum of **5** measured in $CDCl_3$.

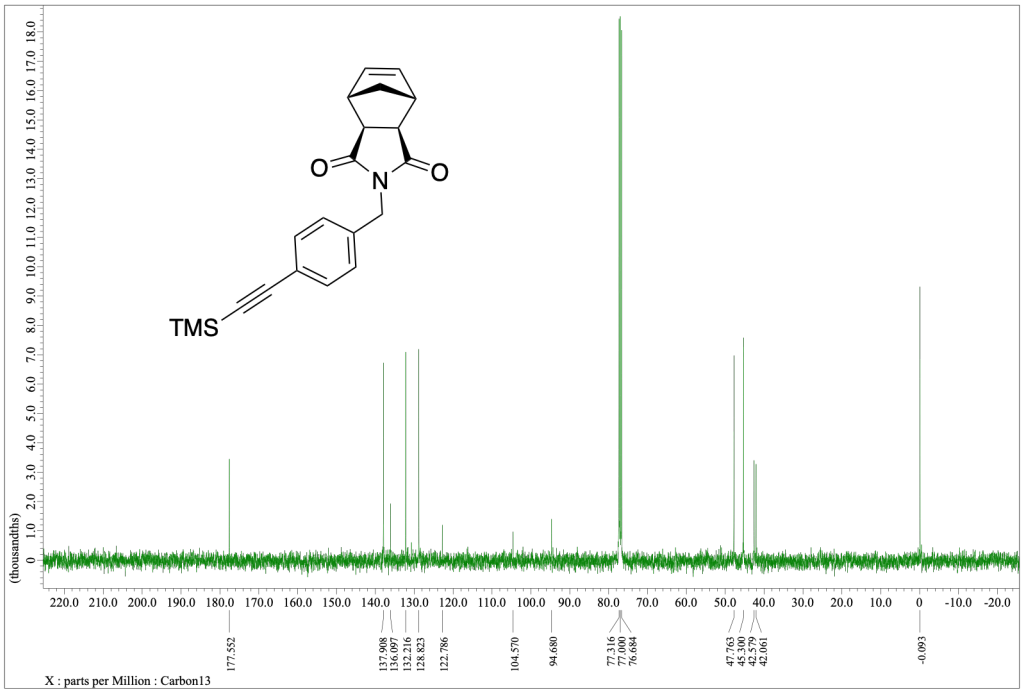

Fig. S3 ^{13}C NMR (100 MHz) spectrum of **5** measured in $CDCl_3$.

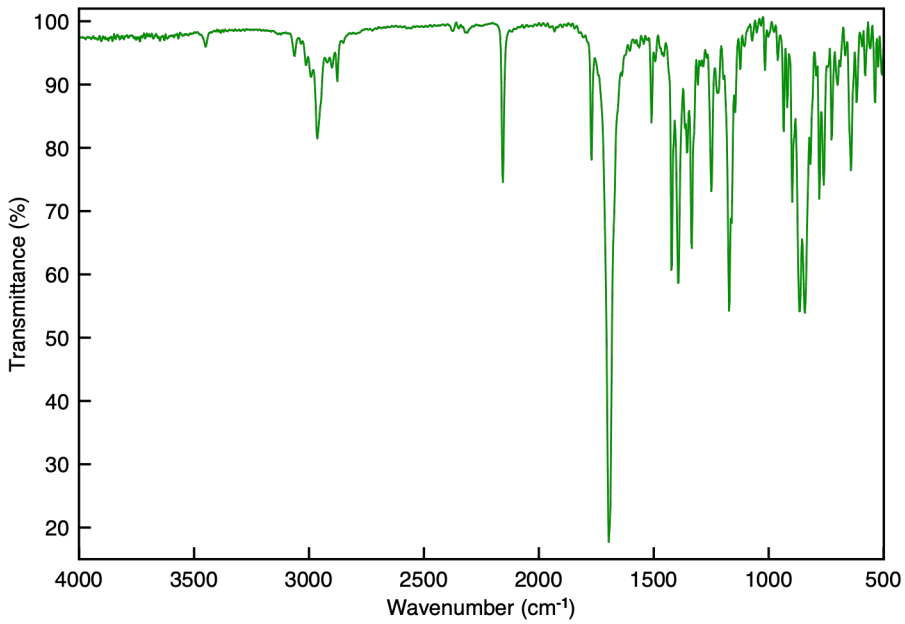

Fig. S4 IR absorption spectrum (KBr pellet) of **5**.

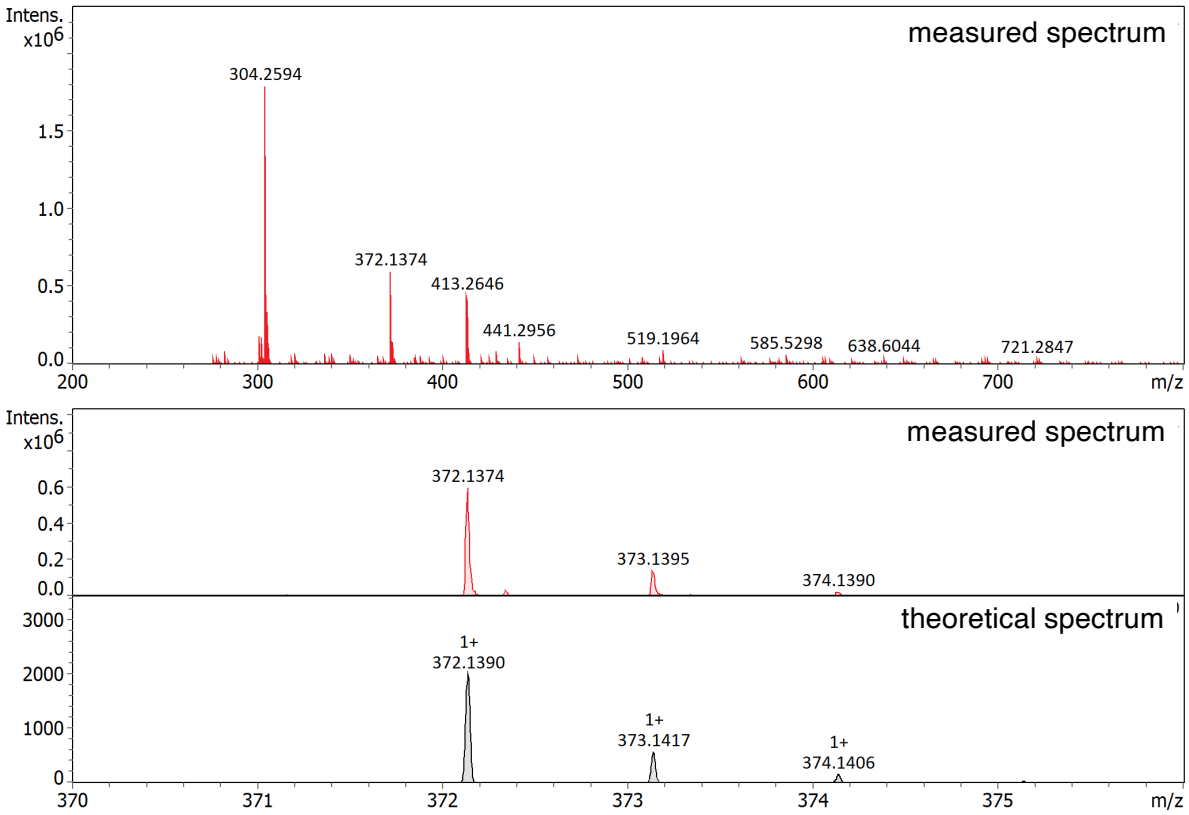

Fig. S5 ESI-MS charts of **5** measured in MeOH.

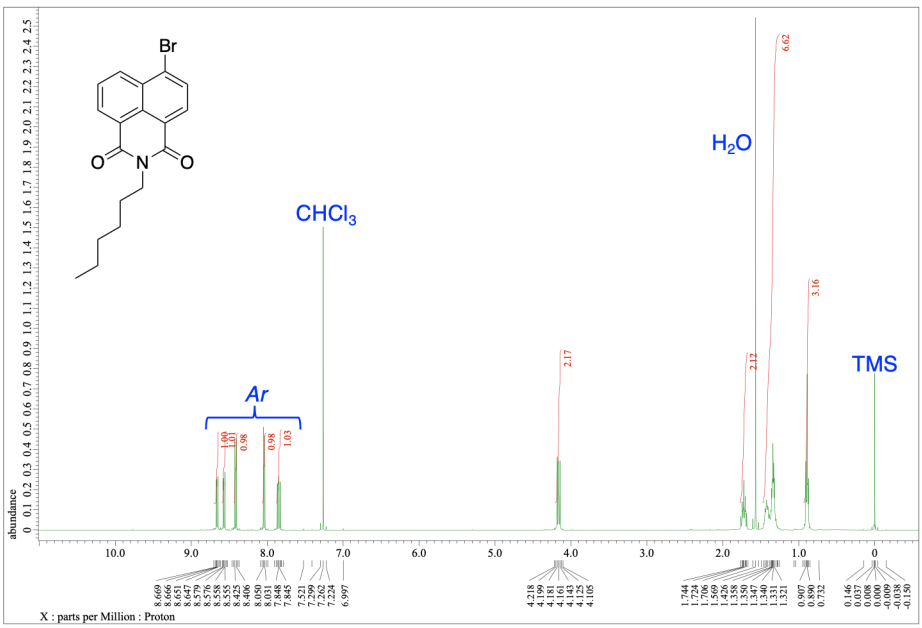

Fig. S6 ^{1}H NMR (400 MHz) spectrum of **6** measured in $CDCl_3$.

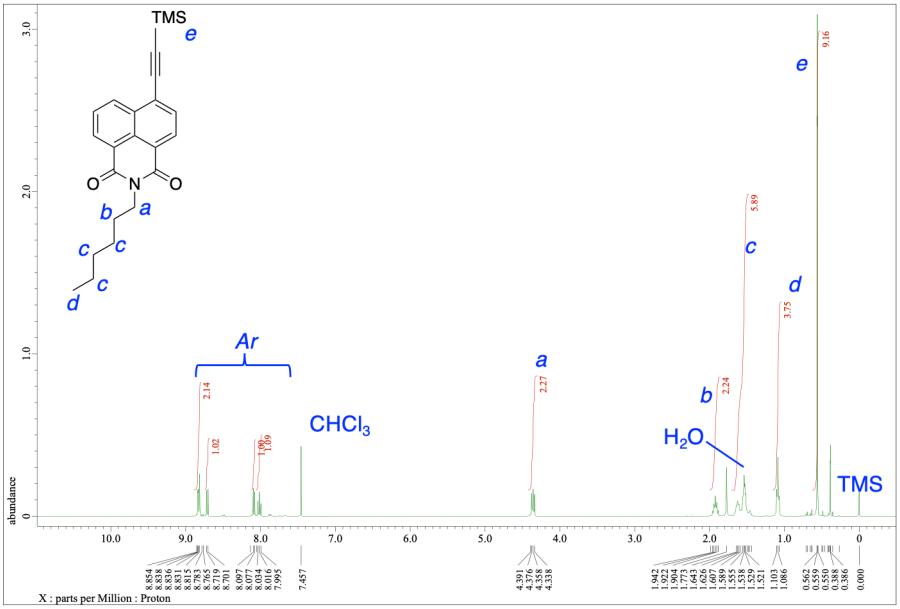

Fig. S7 ^{1}H NMR (400 MHz) spectrum of **7** measured in $CDCl_3$.

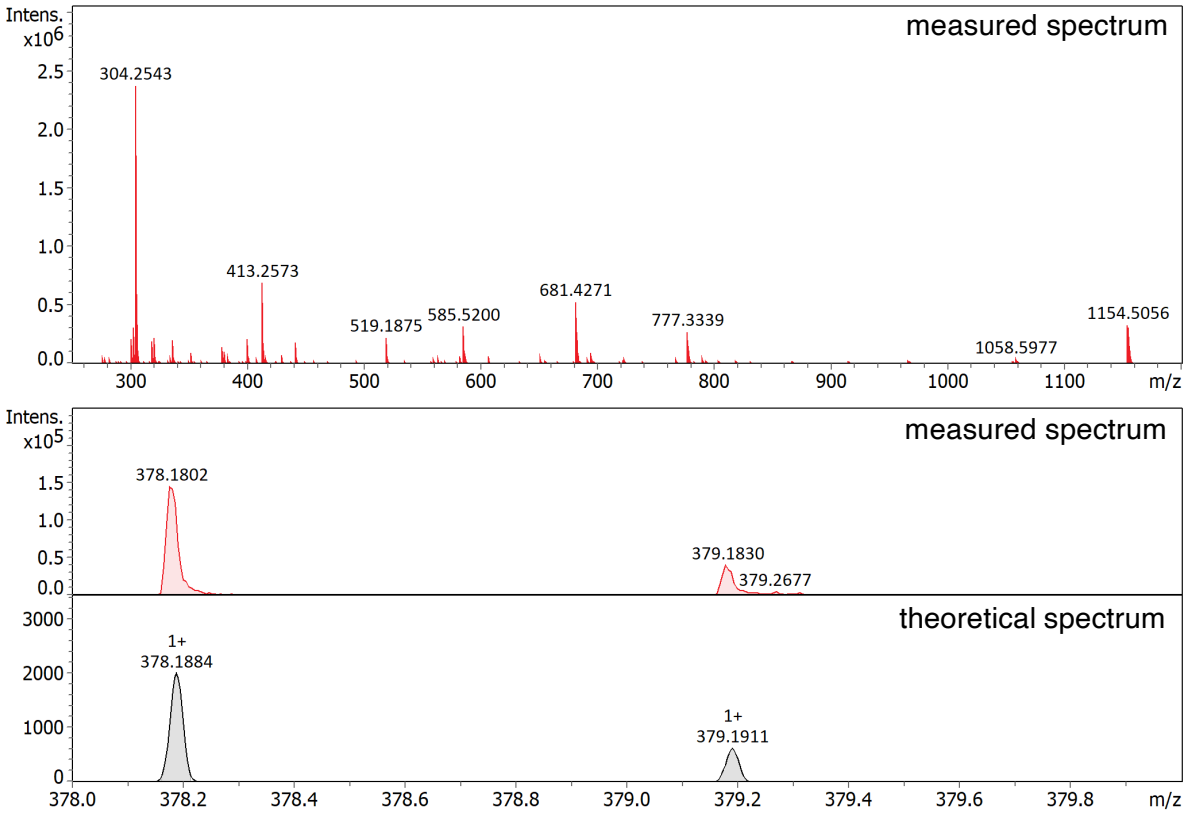

Fig. S8 ESI-MS charts of **7** measured in MeOH.

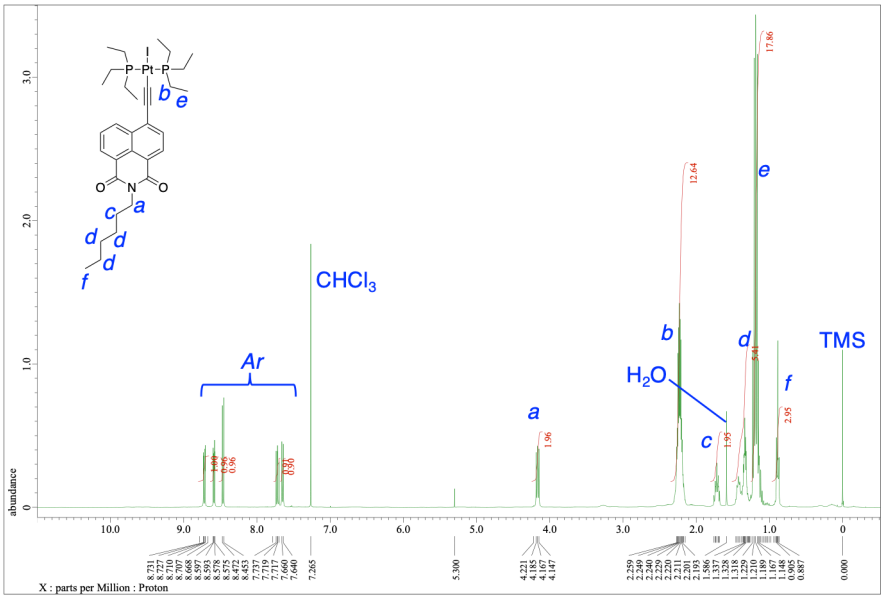

Fig. S9 ^{1}H NMR (400 MHz) spectrum of **8** measured in $CDCl_3$.

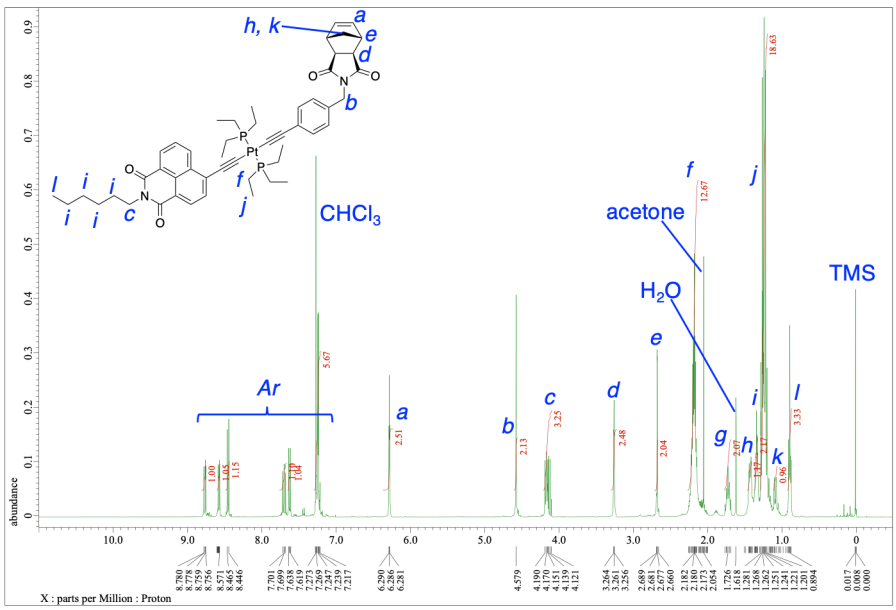

Fig. S10 ^{1}H NMR (400 MHz) spectrum of **1** measured in $CDCl_3$.

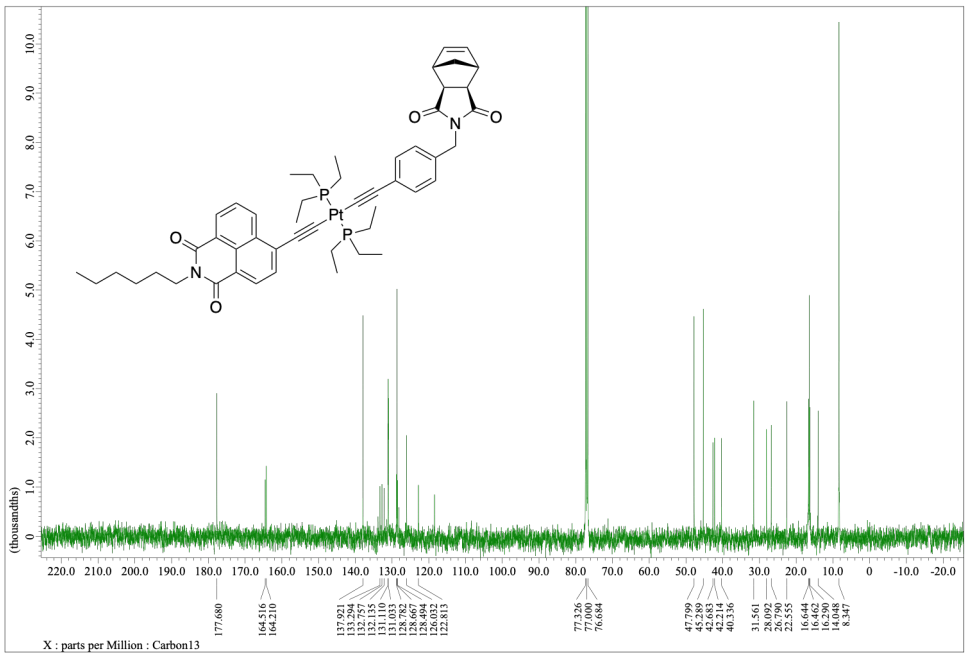

Fig. S11 ^{13}C NMR (100 MHz) spectrum of **1** measured in $CDCl_3$.

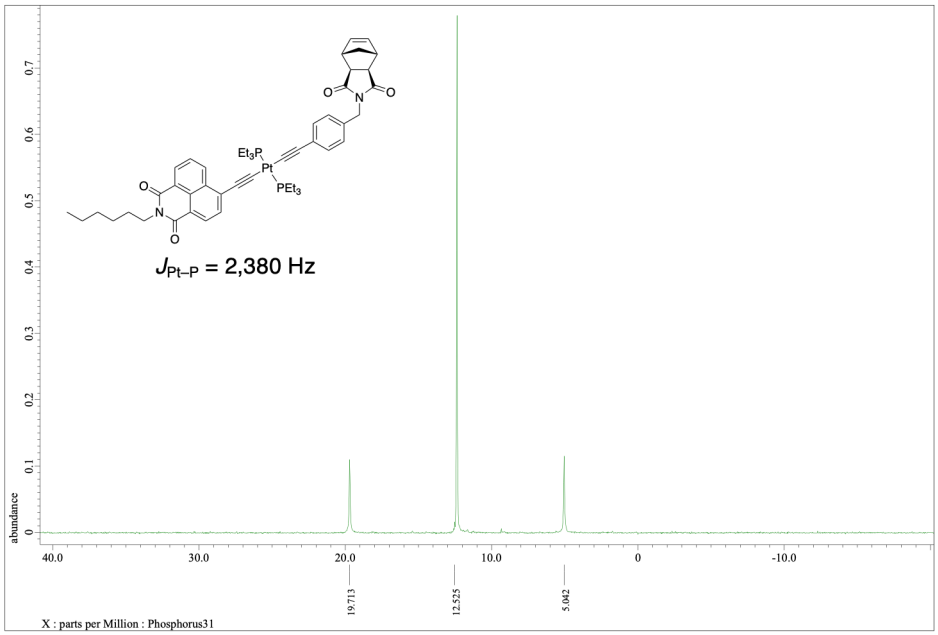

Fig. S12 ^{31}P NMR (162 MHz) spectrum of **1** measured in $CDCl_3$.

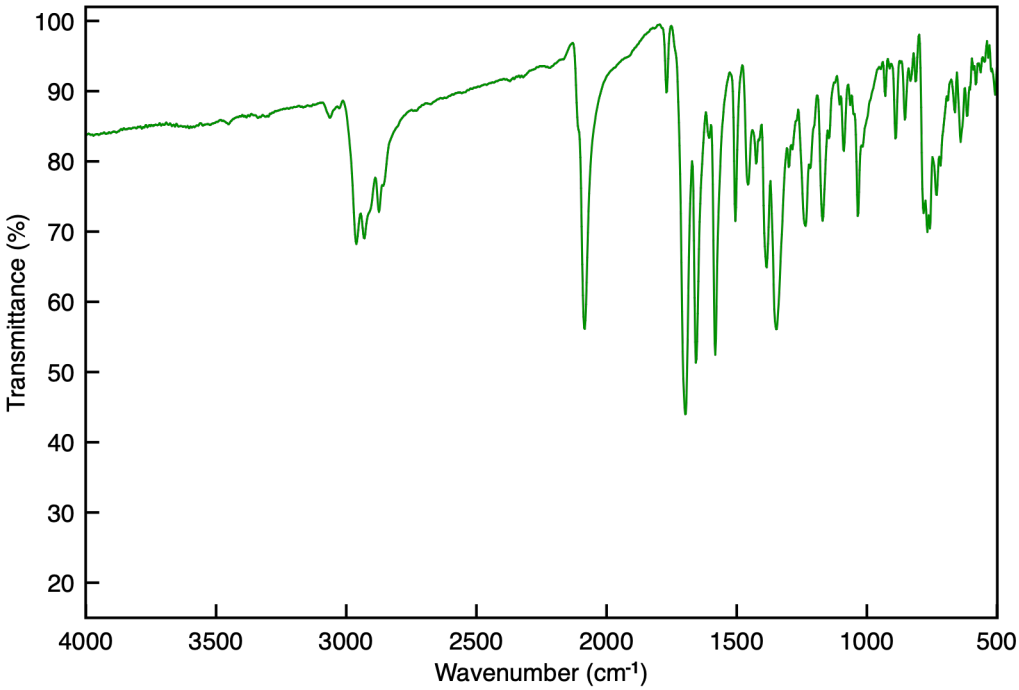

Fig. S13 IR absorption spectrum (KBr pellet) of **1**.

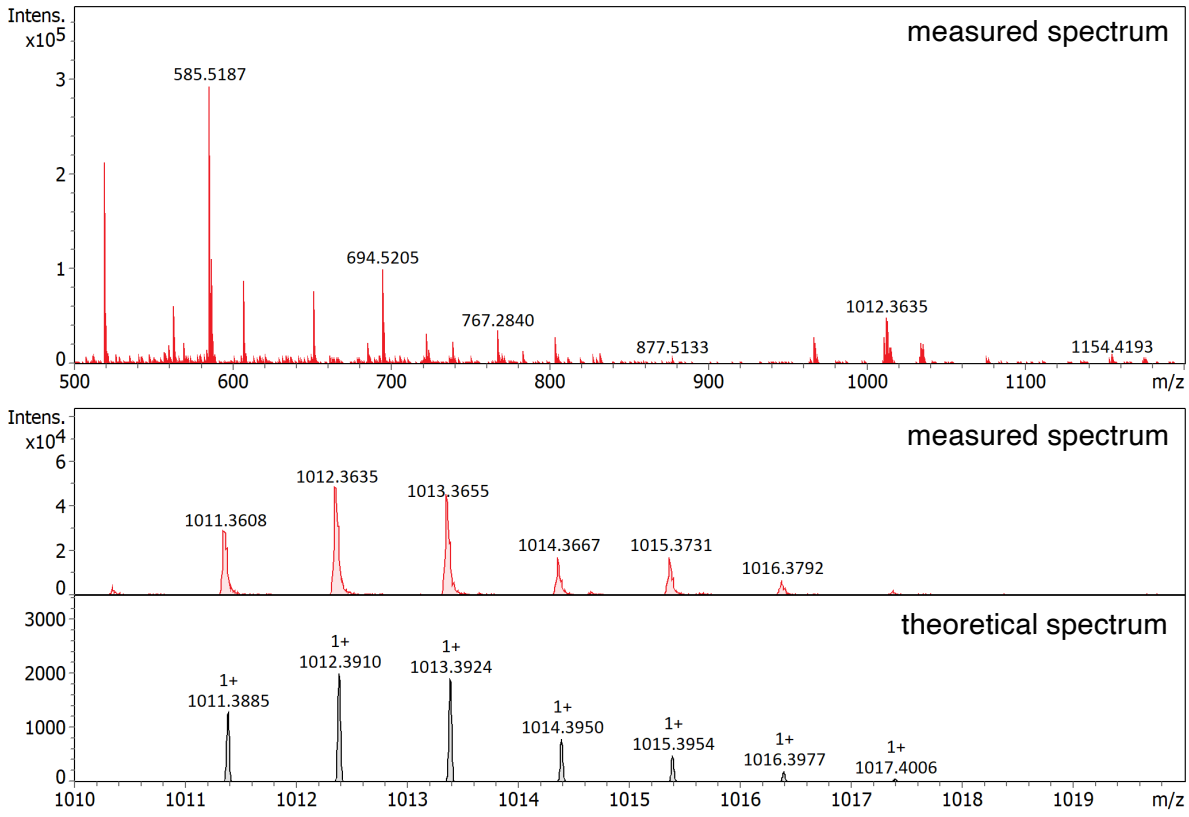

Fig. S14 ESI-MS charts of **1** measured in MeOH.

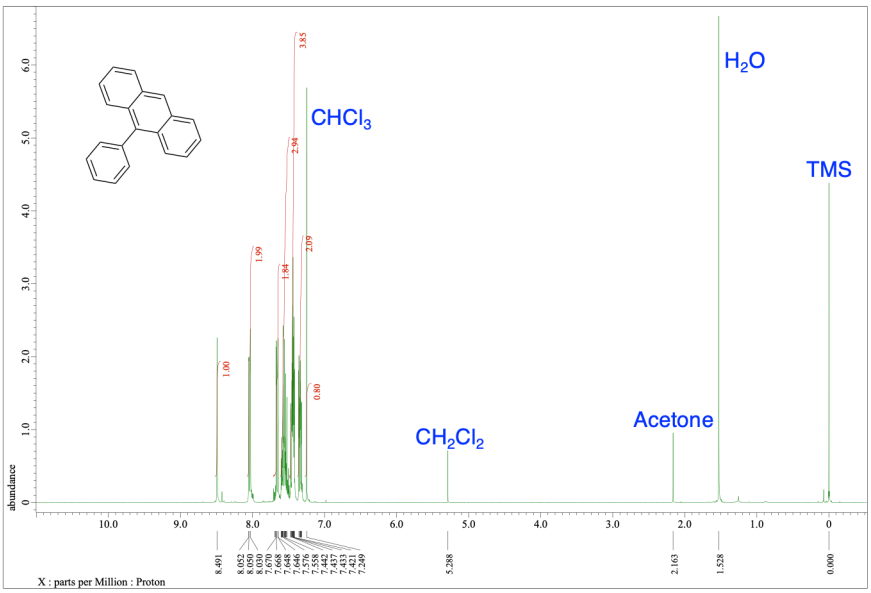

Fig. S15 ^{1}H NMR (400 MHz) spectrum of **9** measured in $CDCl_3$.

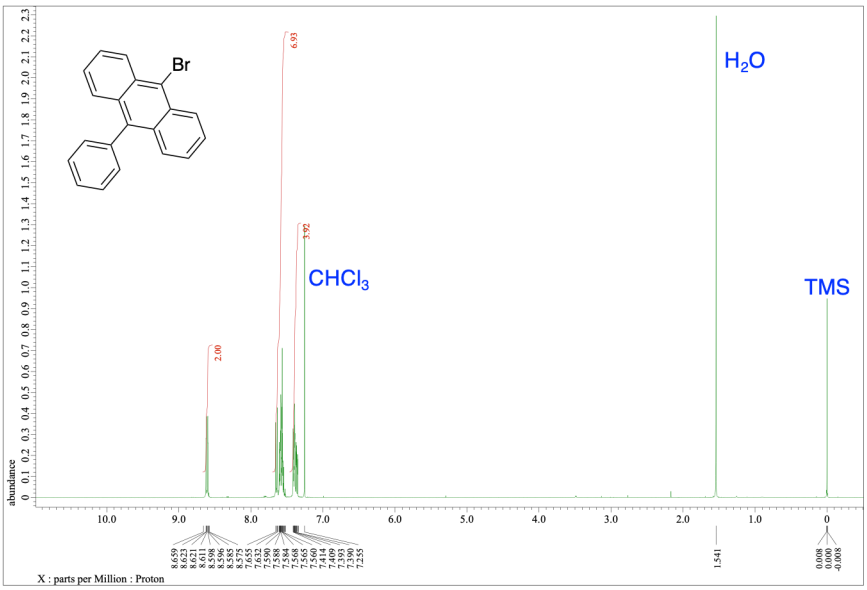

Fig. S16 ^{1}H NMR (400 MHz) spectrum of **10** measured in $CDCl_3$.

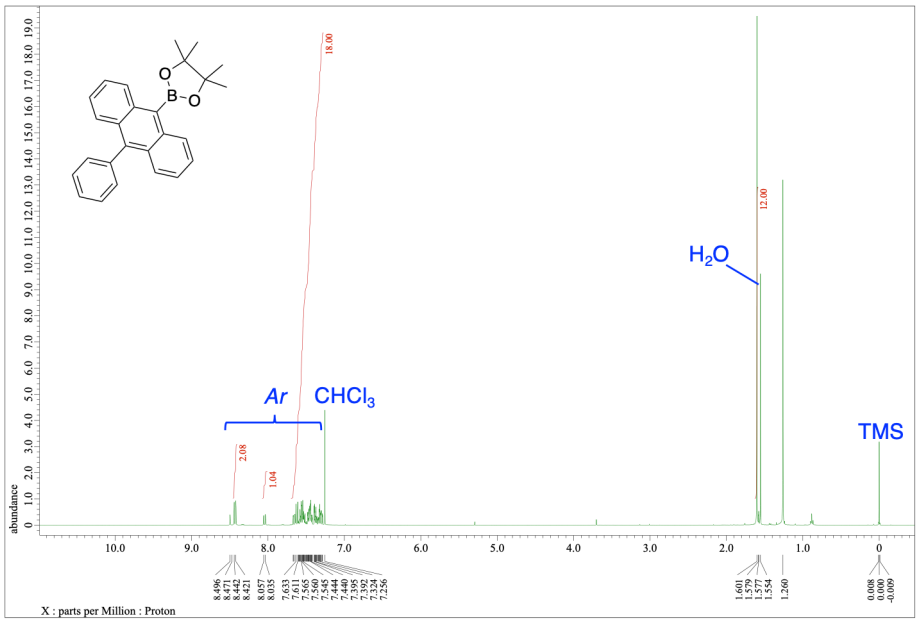

Fig. S17 ^{1}H NMR (400 MHz) spectrum of **11** measured in $CDCl_3$.

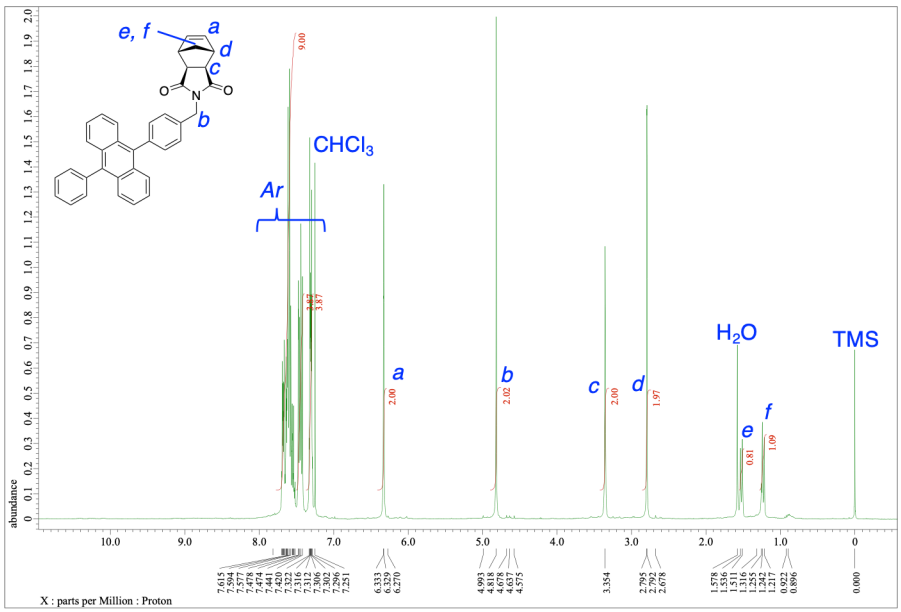

Fig. S18 ^{1}H NMR (400 MHz) spectrum of **2** measured in $CDCl_3$.

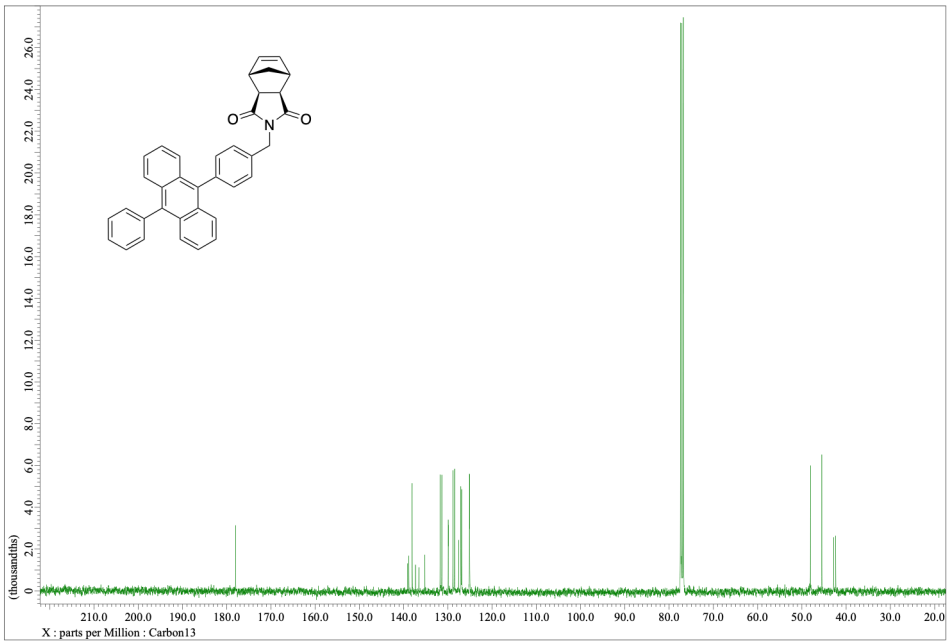

Fig. S19 ^{13}C NMR (100 MHz) spectrum of **2** measured in $CDCl_3$.

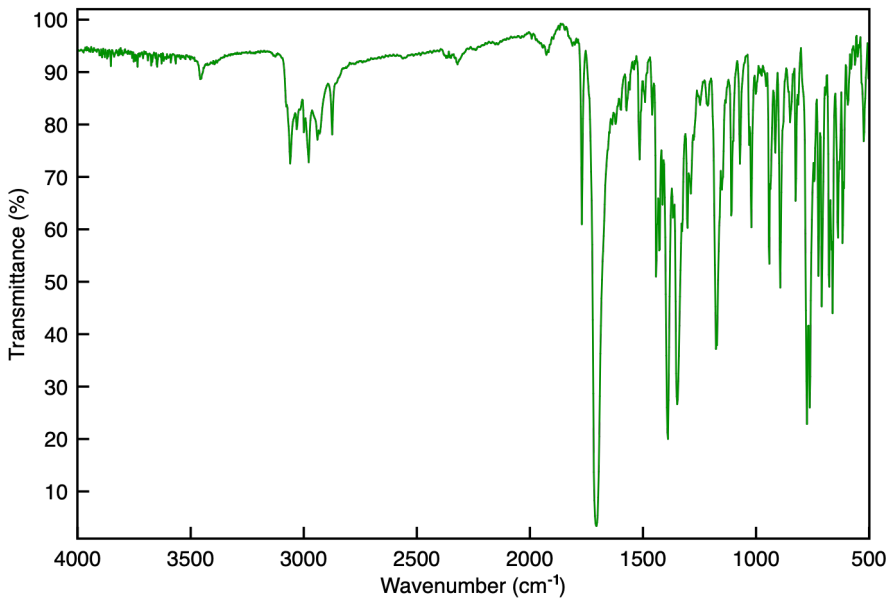

Fig. S20 IR absorption spectrum (KBr pellet) of **2**.

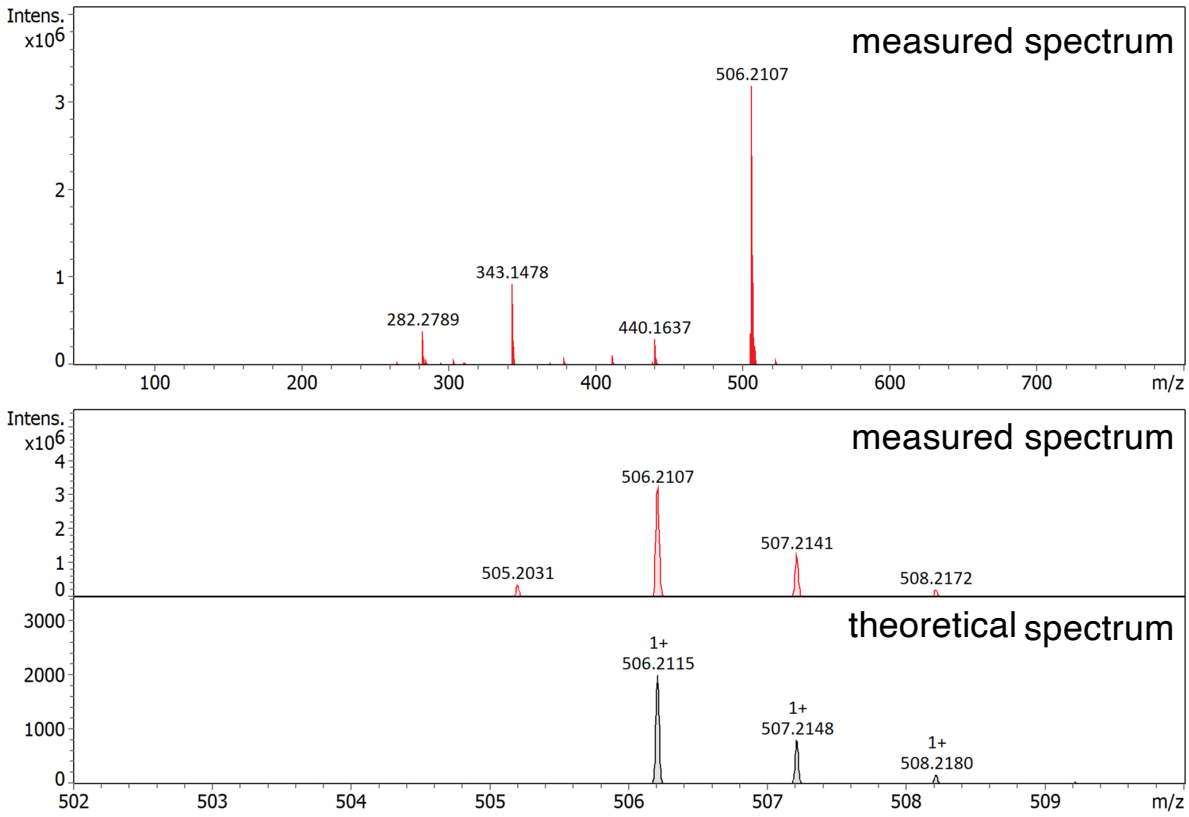

Fig. S21 ESI-MS charts of **2** measured in MeOH.

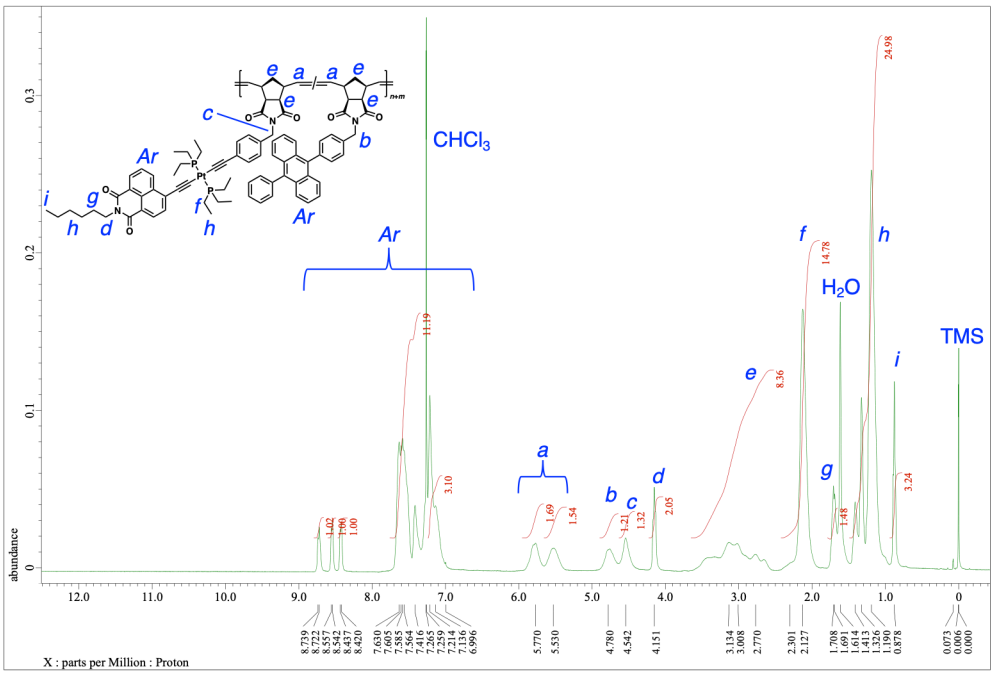

Fig. S22 ^{1}H NMR (400 MHz) spectrum of poly(**1**$_{50}$-*co*-**2**$_{50}$) measured in $CDCl_3$.

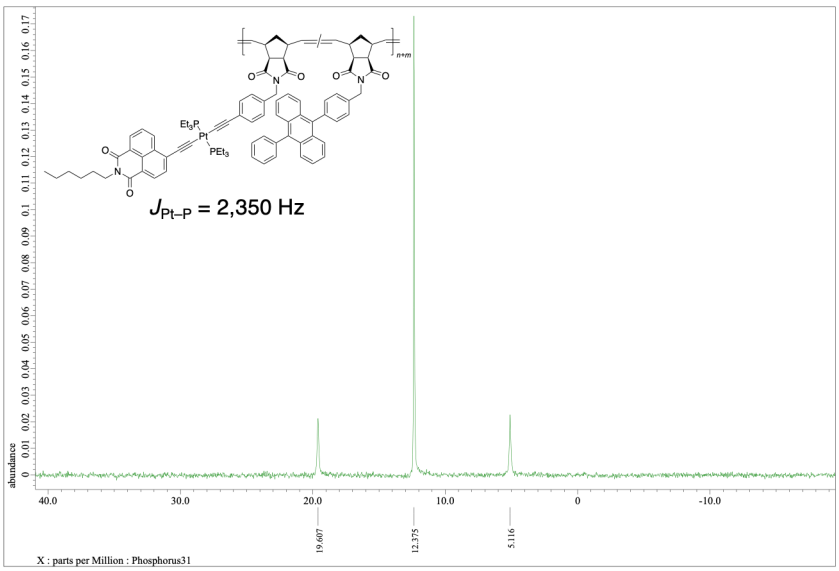

Fig. S23 ^{31}P NMR (162 MHz) spectrum of poly(**1**$_{50}$-*co*-**2**$_{50}$) measured in $CDCl_3$.

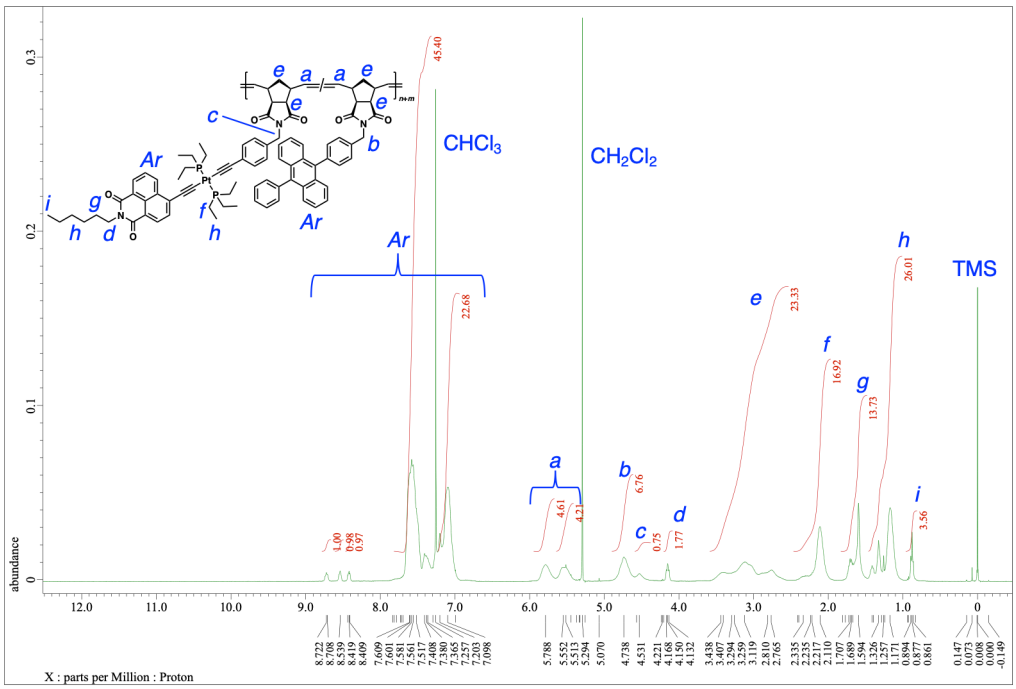

Fig. S24 ^{1}H NMR (400 MHz) spectrum of poly(**1**$_{20}$-*co*-**2**$_{100}$) measured in $CDCl_3$.

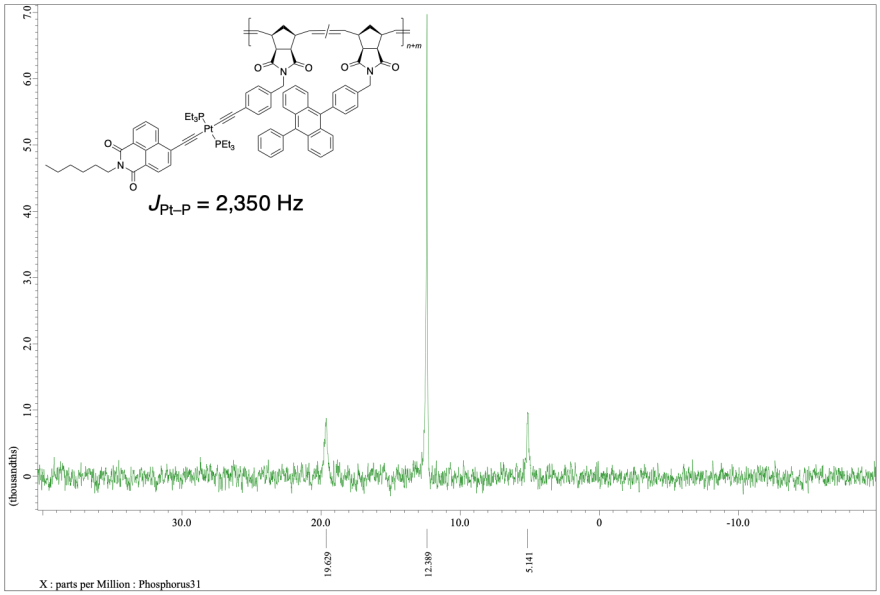

Fig. S25 ^{31}P NMR (162 MHz) spectrum of poly(**1**$_{20}$-*co*-**2**$_{100}$) measured in $CDCl_3$.

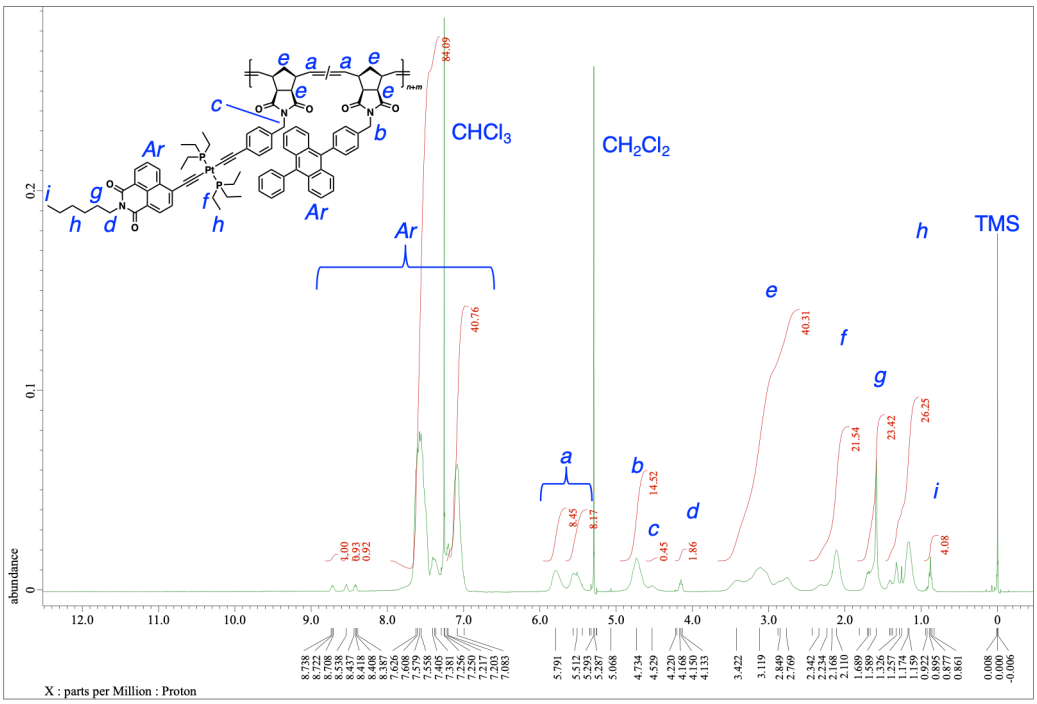

Fig. S26 ^{1}H NMR (400 MHz) spectrum of poly(**1**$_{10}$-*co*-**2**$_{100}$) measured in $CDCl_3$.

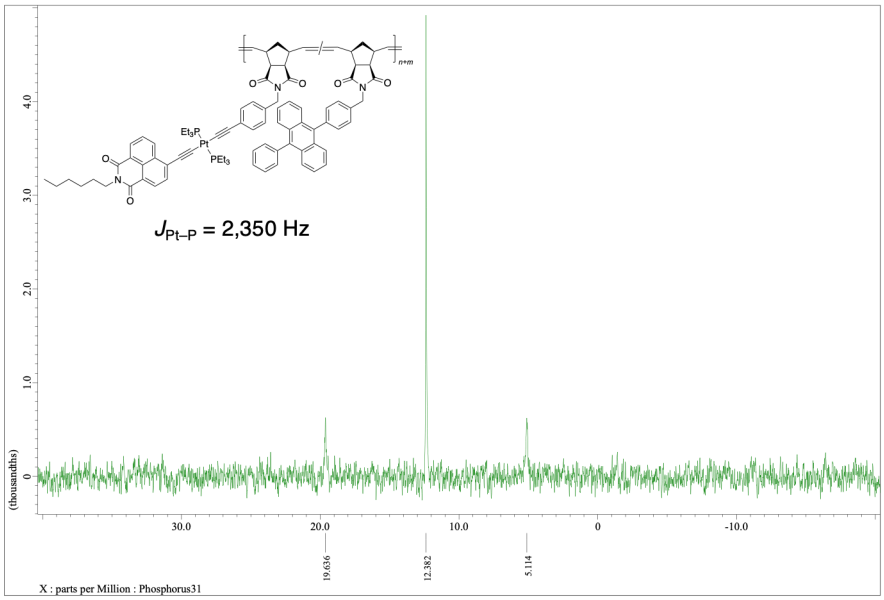

Fig. S27 ^{31}P NMR (162 MHz) spectrum of poly(**1**$_{10}$-*co*-**2**$_{100}$) measured in $CDCl_3$.

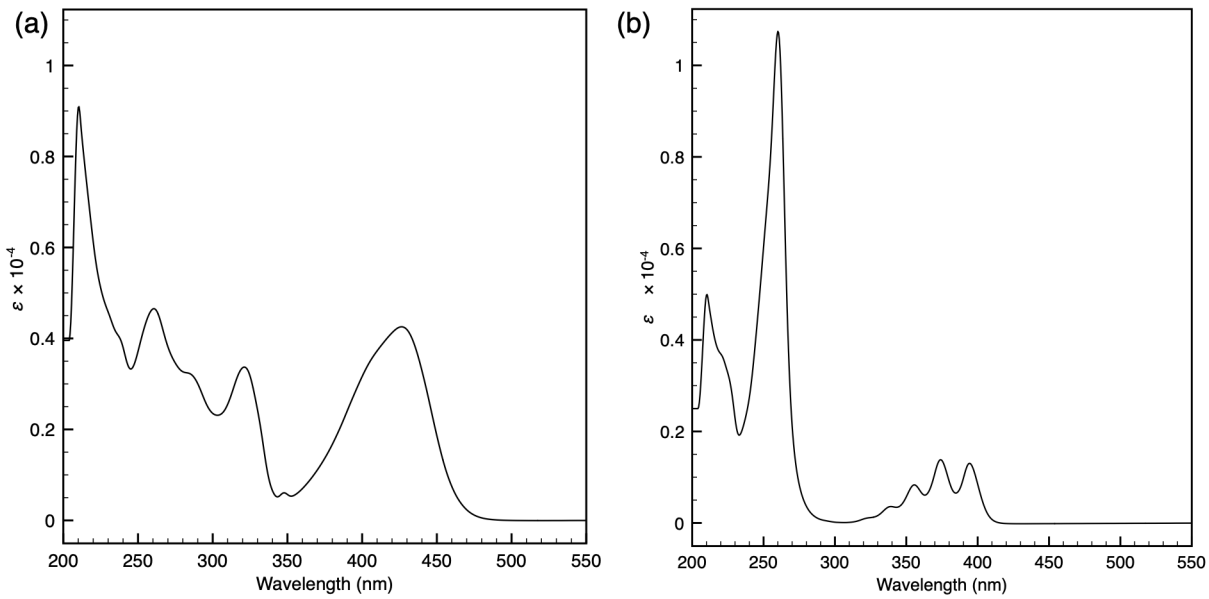

Fig. S28 UV–vis absorption spectra of (a) **1** and (b) **2** measured in THF (c = 0.01 mM).

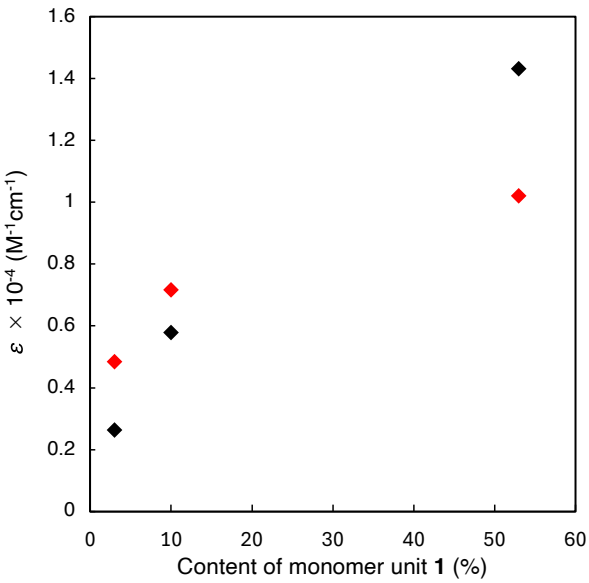

Fig. S29 Dependence of ε values at 427 nm (black diamond) and 396.5 nm (red diamond) on the content of **1** (see Table 1) in poly(**1**$_{50}$-*co*-**2**$_{50}$), poly(**1**$_{20}$-*co*-**2**$_{100}$) and poly(**1**$_{10}$-*co*-**2**$_{100}$) measured in THF (c = 0.01 mM).

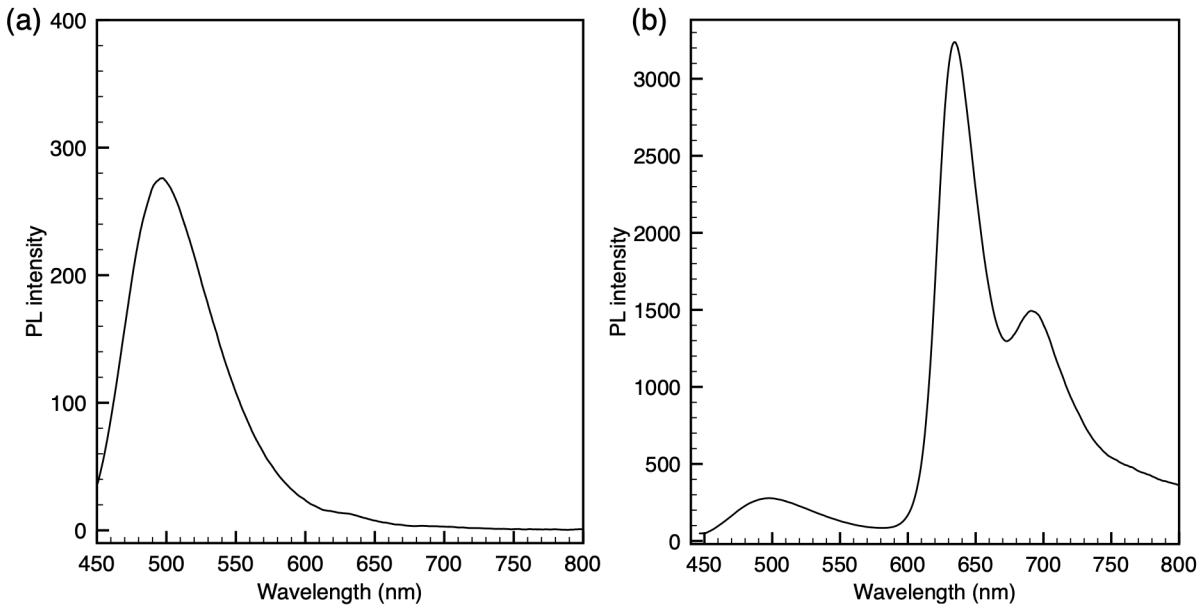

Fig. S30 PL spectra of **1** excited at 426.5 nm measured in THF (c = 0.01 mM) under (a) air and (b) N_2.

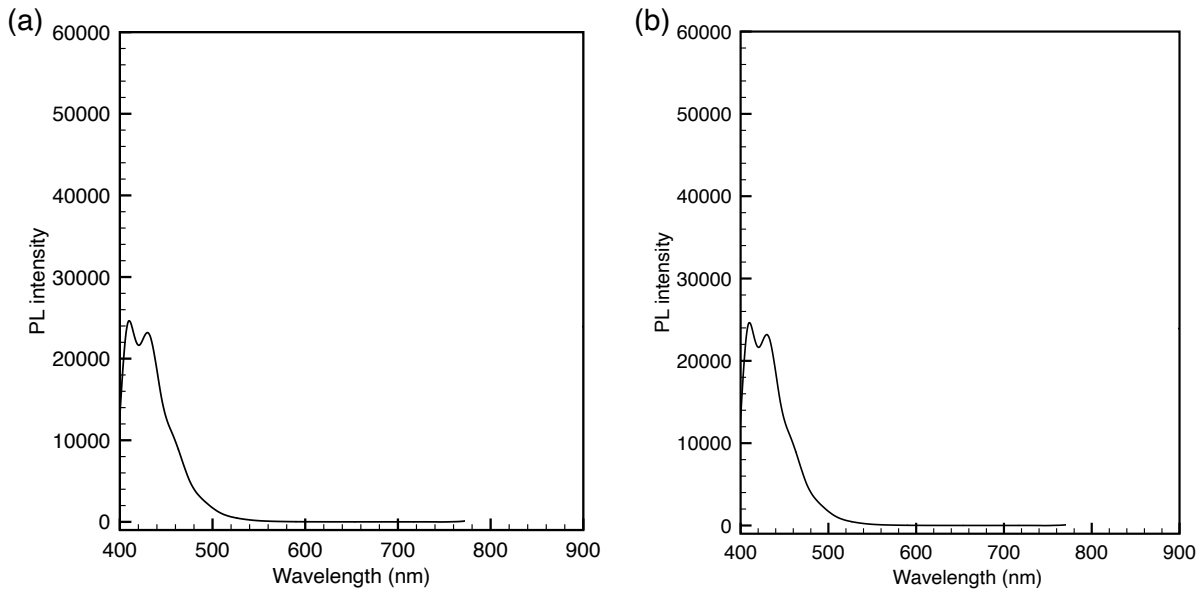

Fig. S31 PL spectra of **2** excited at 374 nm measured in THF (c = 0.01 mM) under (a) air and (b) N_2.

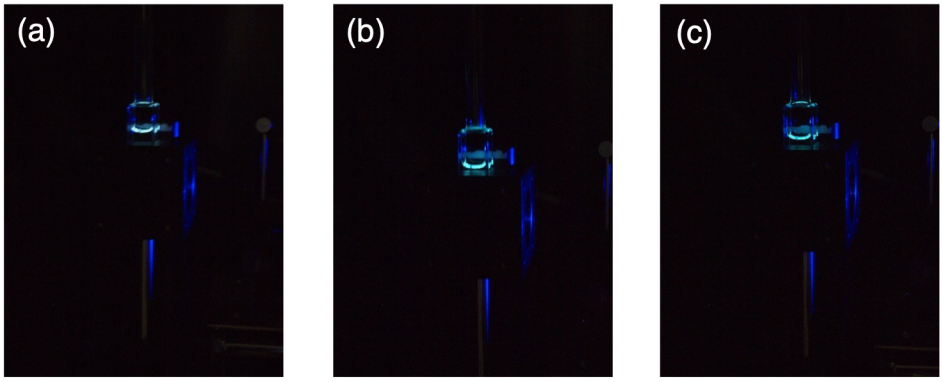

Fig. S32 Photographs of the solutions of (a) poly(**1**$_{50}$-*co*-**2**$_{50}$), (b) poly(**1**$_{20}$-*co*-**2**$_{100}$), and (c) poly(**1**$_{10}$-*co*-**2**$_{100}$) in the experiment of Fig. 8a.

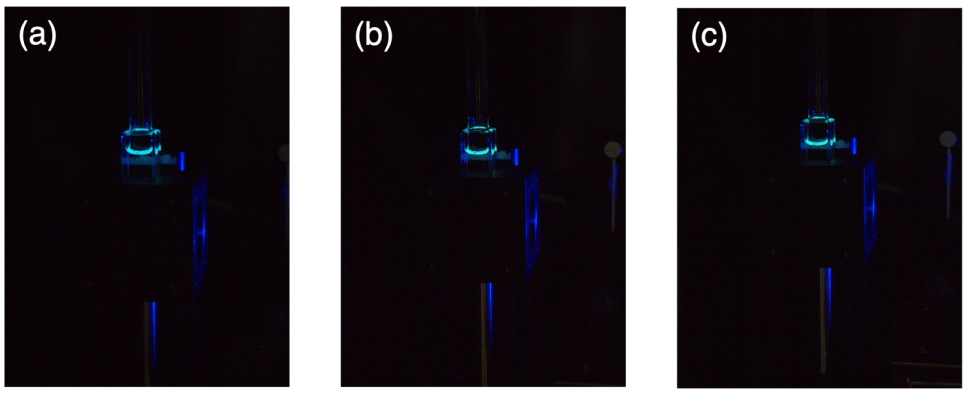

Fig. S33 Photographs of the solutions of (a) poly(**1**$_{50}$-*co*-**2**$_{50}$)/DPA, (b) poly(**1**$_{20}$-*co*-**2**$_{100}$)/DPA, and (c) poly(**1**$_{10}$-*co*-**2**$_{100}$)/DPA in the experiment of Fig. 8b.

Table S1 Absorption and emission data of the copolymers

Sample	Solvent	Sample conc. (mM)	DPA conc. (mM)	A [b]	E [b]	η_{UC} [c] (%)
poly(**1**$_{50}$-*co*-**2**$_{50}$)	THF	0.04	0.24	0.12	15.5	7.6
poly(**1**$_{20}$-*co*-**2**$_{100}$)	THF	0.12	0.24	0.19	2.2	0.66
poly(**1**$_{10}$-*co*-**2**$_{100}$)	THF	0.22	0.24	0.16	0.55	0.20
DCM [a]	MeOH	0.001	–	0.048	66.7	–

[a] 4-(Dicyanomethylene)-2-methyl-6-(4-dimethylaminostyryl)-4*H*-pyran, employed as a reference. [b] See below. [c] Calculated using an equation,[S8]

$$\eta_{UC} = 2\phi_R \frac{I_R A_R E_s \eta_S^2}{I_S A_S E_R \eta_R^2}$$

wherein Φ_R is the quantum yield of fluorescence of DCM (35% in methanol, Exciton), I_S: intensity of excitation light for a sample solution, A_S: absorbance of a sample solution at 450 nm, E_S: adjusted integral of emission between 350 and 450 nm from a sample upon irradiation of blue light (λ = 450 nm), η_S: refractive index of a sample solution, I_R: intensity of excitation light for a reference solution, A_R: absorbance of a reference solution at 450 nm, E_R: adjusted integral of emission from a reference solution upon irradiation of blue light (λ = 450 nm), η_R: refractive index of a reference solution. The intensity of excitation light was 4.7 mW (47 mW/cm^2) for the measurement of the samples and reference.

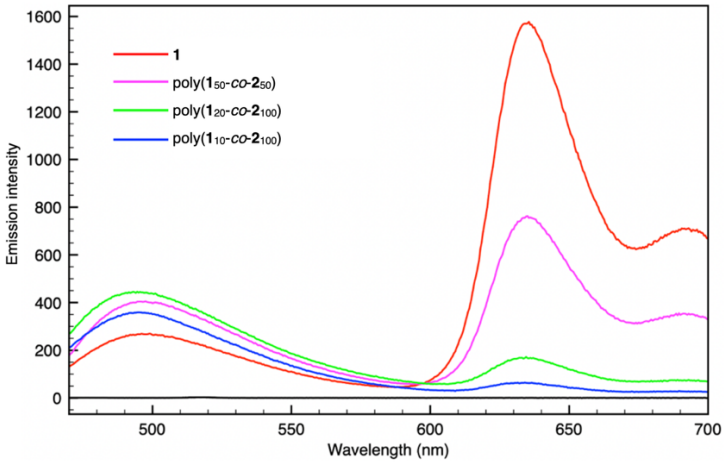

Fig. S34 PL spectra of **1** and the copolymers excited at 450 nm measured in THF under N_2, *c* of Pt unit = 0.02 mM.

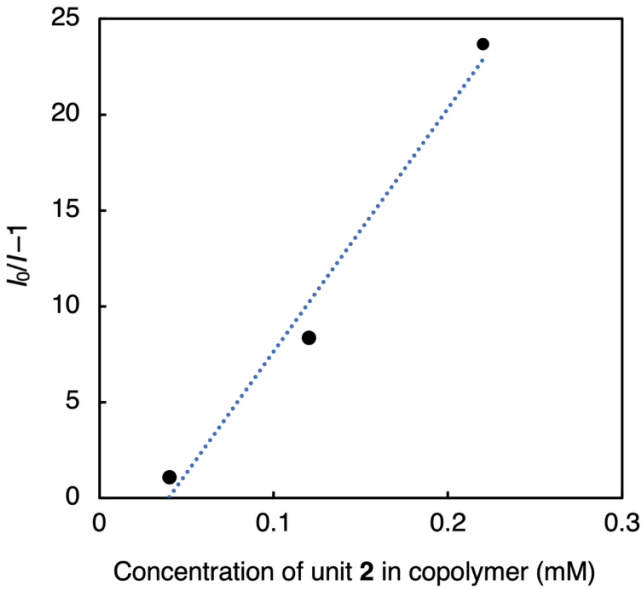

Fig. S35 Stern–Volmer plots for poly(**1**$_{50}$-*co*-**2**$_{50}$), poly(**1**$_{10}$-*co*-**2**$_{100}$) and poly(**1**$_{20}$-*co*-**2**$_{100}$) regarding unit **1** as a sensitizer and unit **2** as an emitter, exited at 450 nm measured in THF (*c* of Pt unit = 0.02 mM) under N_2. The PL intensity was determined at 640 nm (Fig. S34). I_0 and I are PL intensities of **1** and the copolymers, respectively. $R^2 = 0.981$.

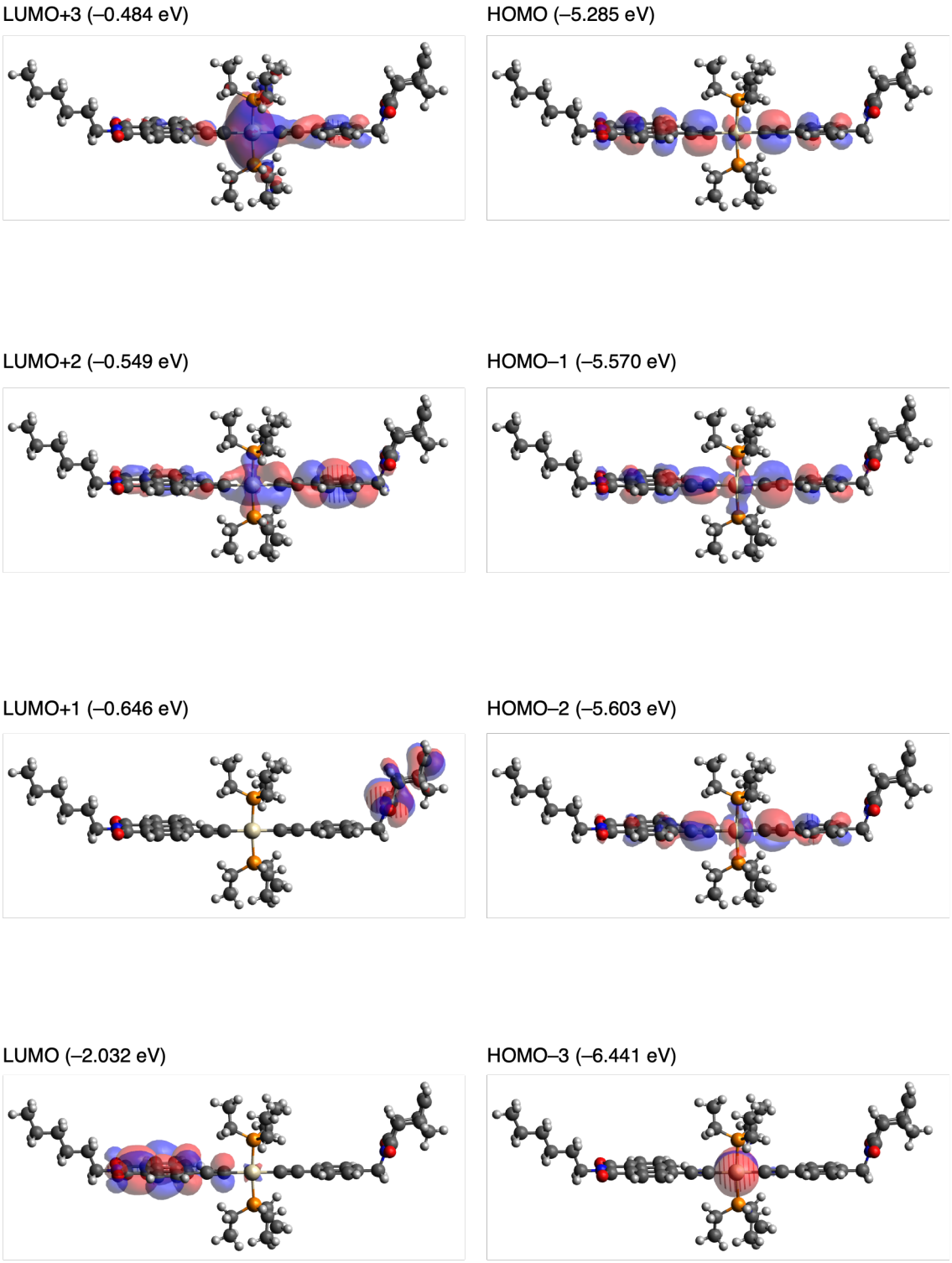

Fig. S36 Shapes and energy levels from LUMO+3 to HOMO–3 of **1** at the ground state obtained by the DFT calculation [B3LYP/6-31G* (H, C, N, O, P), LANL2DZ (Pt)].

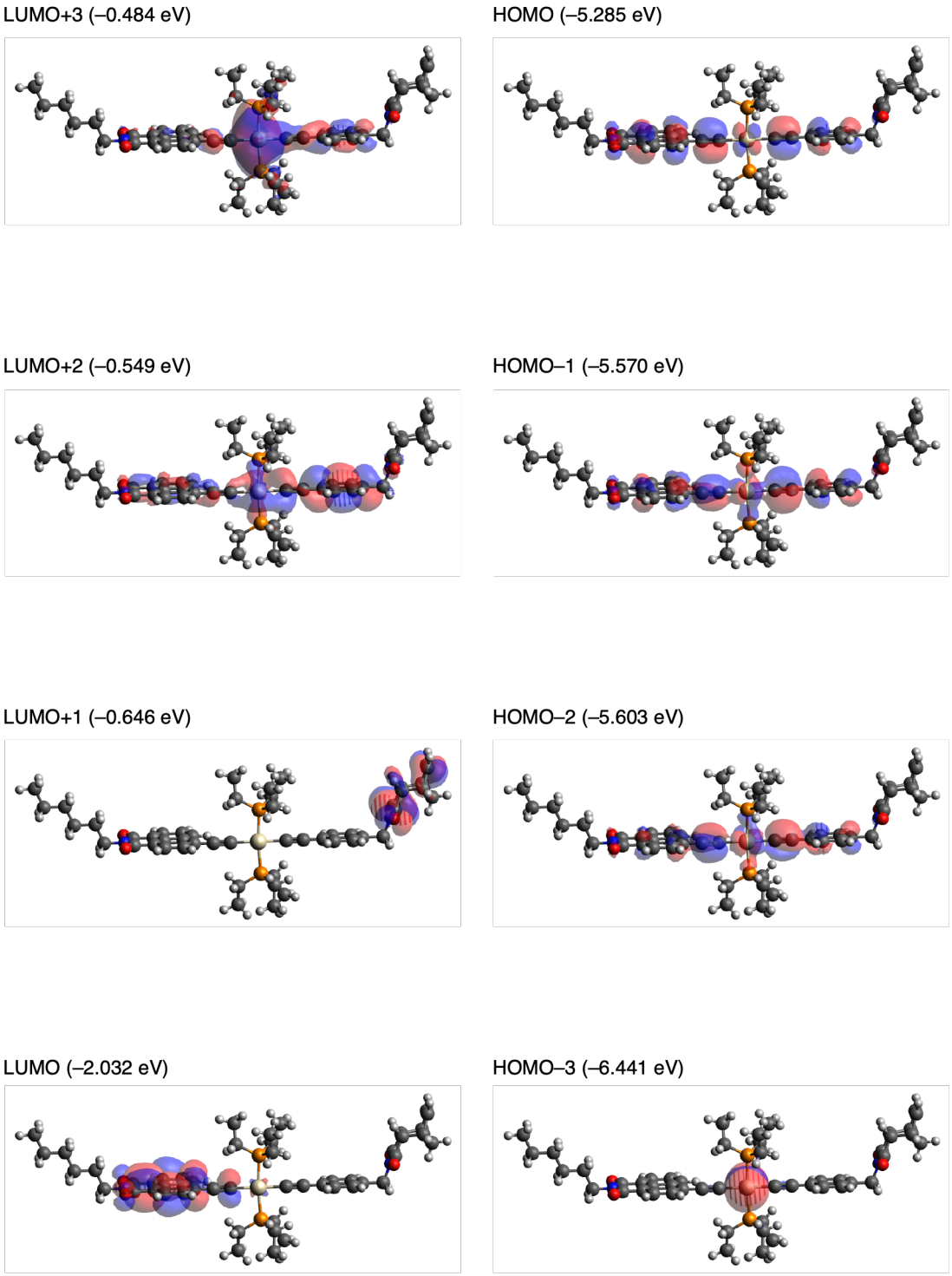

Fig. S37 Shapes and energy levels from LUMO+3 to HOMO–3 of **1** at the ground state obtained by the TD-DFT calculation [B3LYP/6-31G* (H, C, N, O, P), LANL2DZ (Pt), nstates = 40], corresponding to UV–vis absorption.

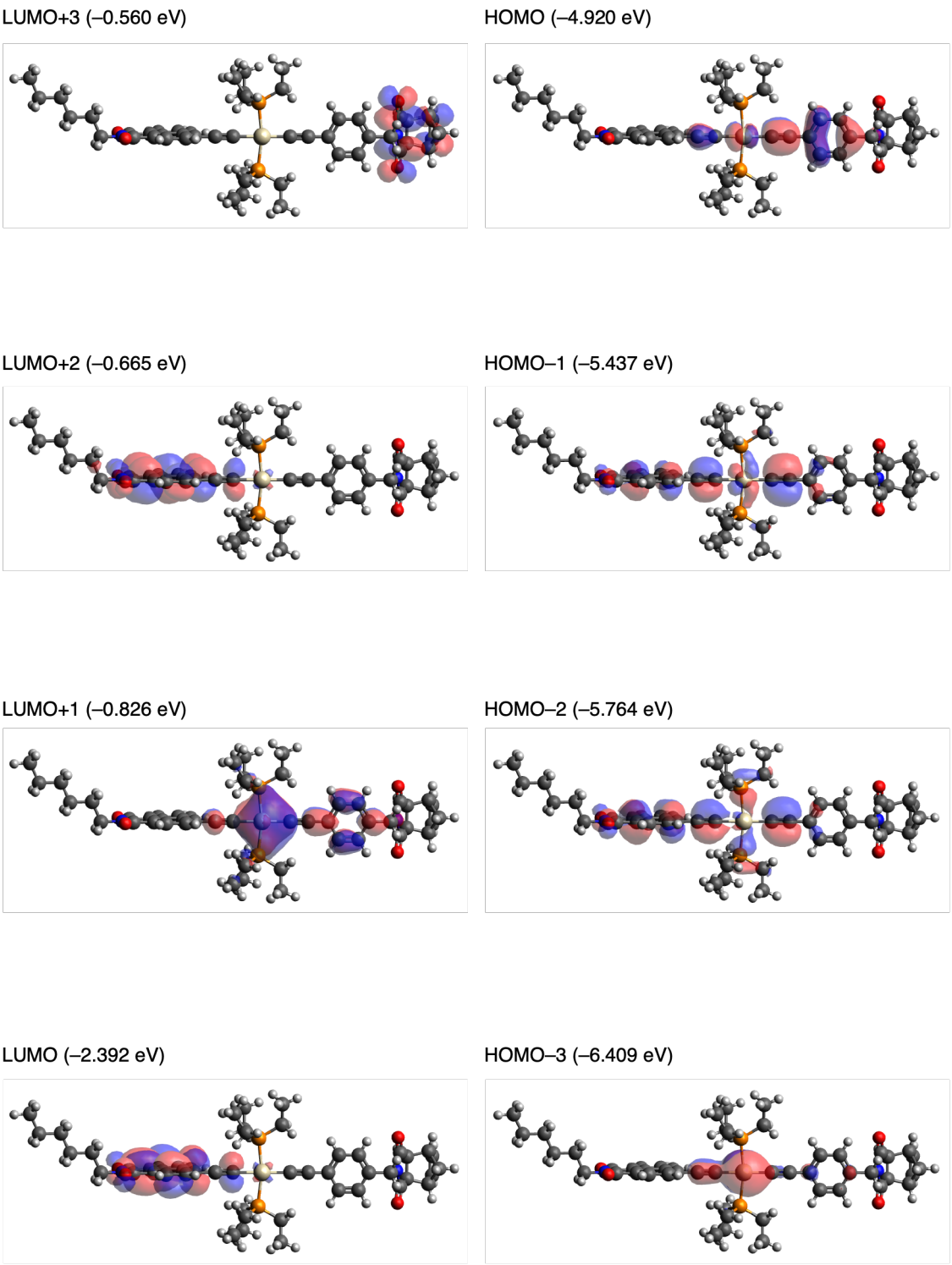

Fig. S38 Shapes and energy levels from LUMO+3 to HOMO–3 of **1** at the excited singlet state obtained by the TD-DFT calculation [B3LYP/6-31G* (H, C, N, O, P), LANL2DZ (Pt), nstates = 40], corresponding to fluorescence emission.

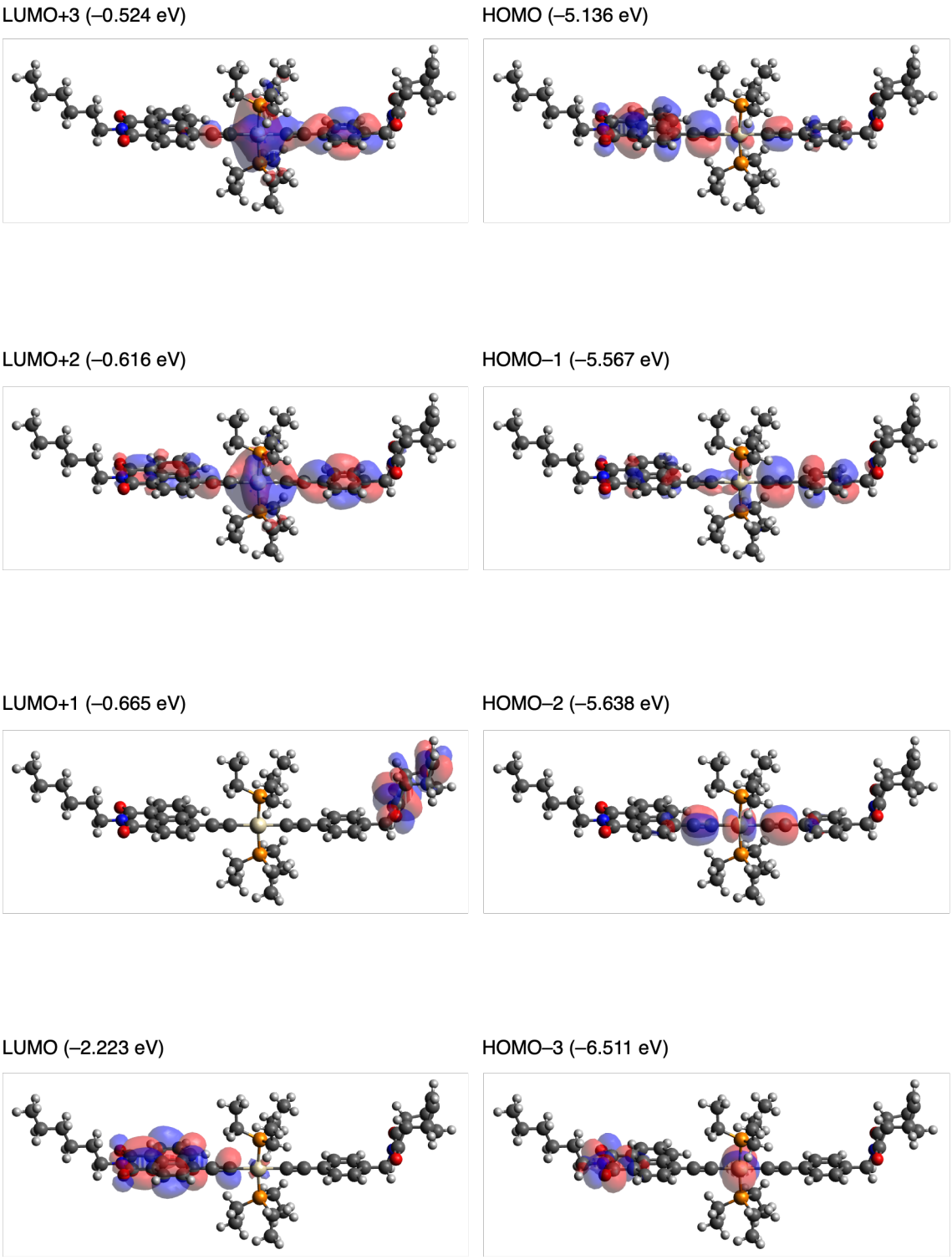

Fig. S39 Shapes and energy levels from LUMO+3 to HOMO–3 of **1** at the excited triplet state obtained by the TD-DFT calculation [B3LYP/6-31G* (H, C, N, O, P), LANL2DZ (Pt), nstates = 40], corresponding to phosphorescence emission.

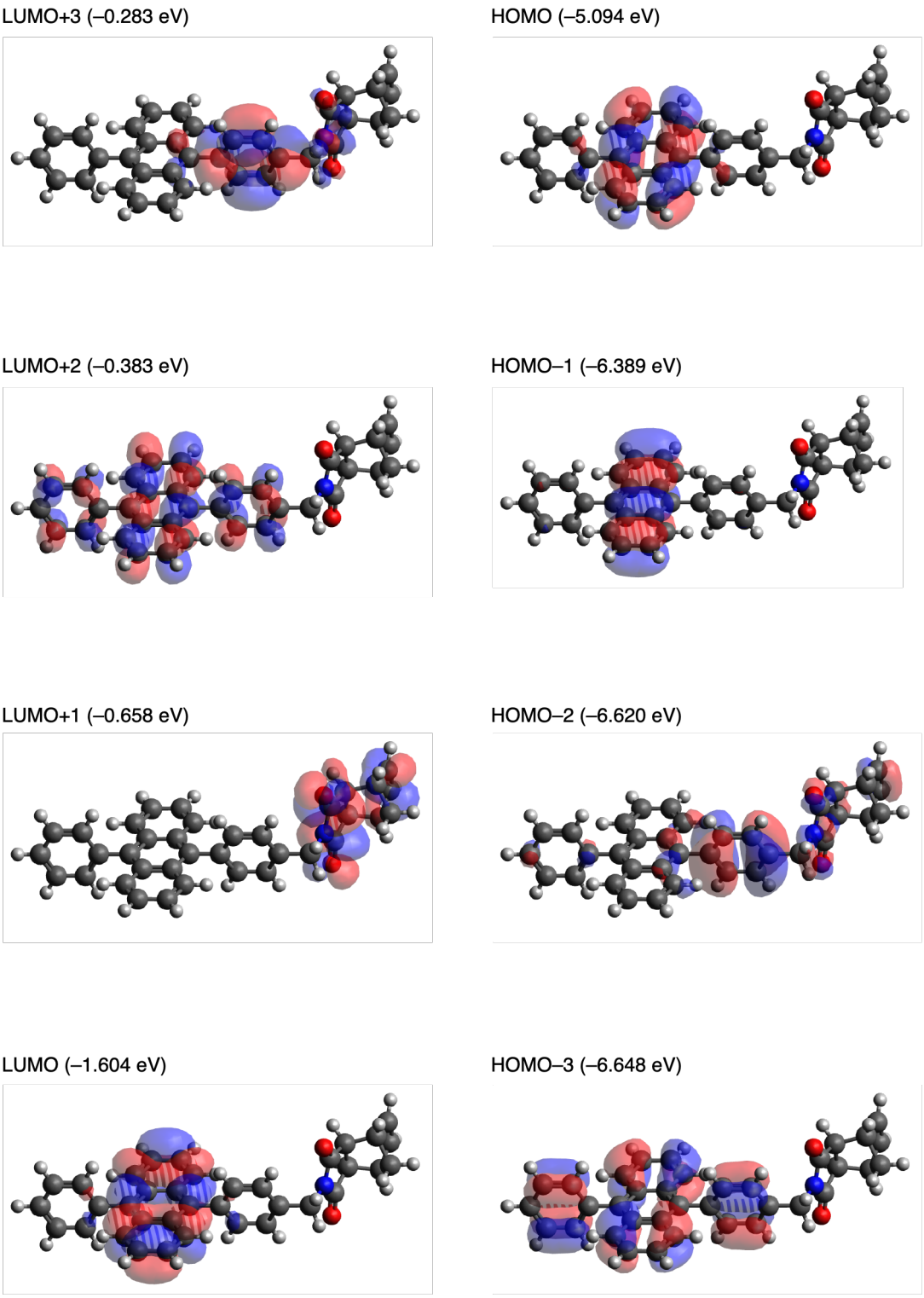

Fig. S40 Shapes and energy levels from LUMO+3 to HOMO–3 of **2** at the ground state obtained by the DFT calculation (B3LYP/6-31G*).

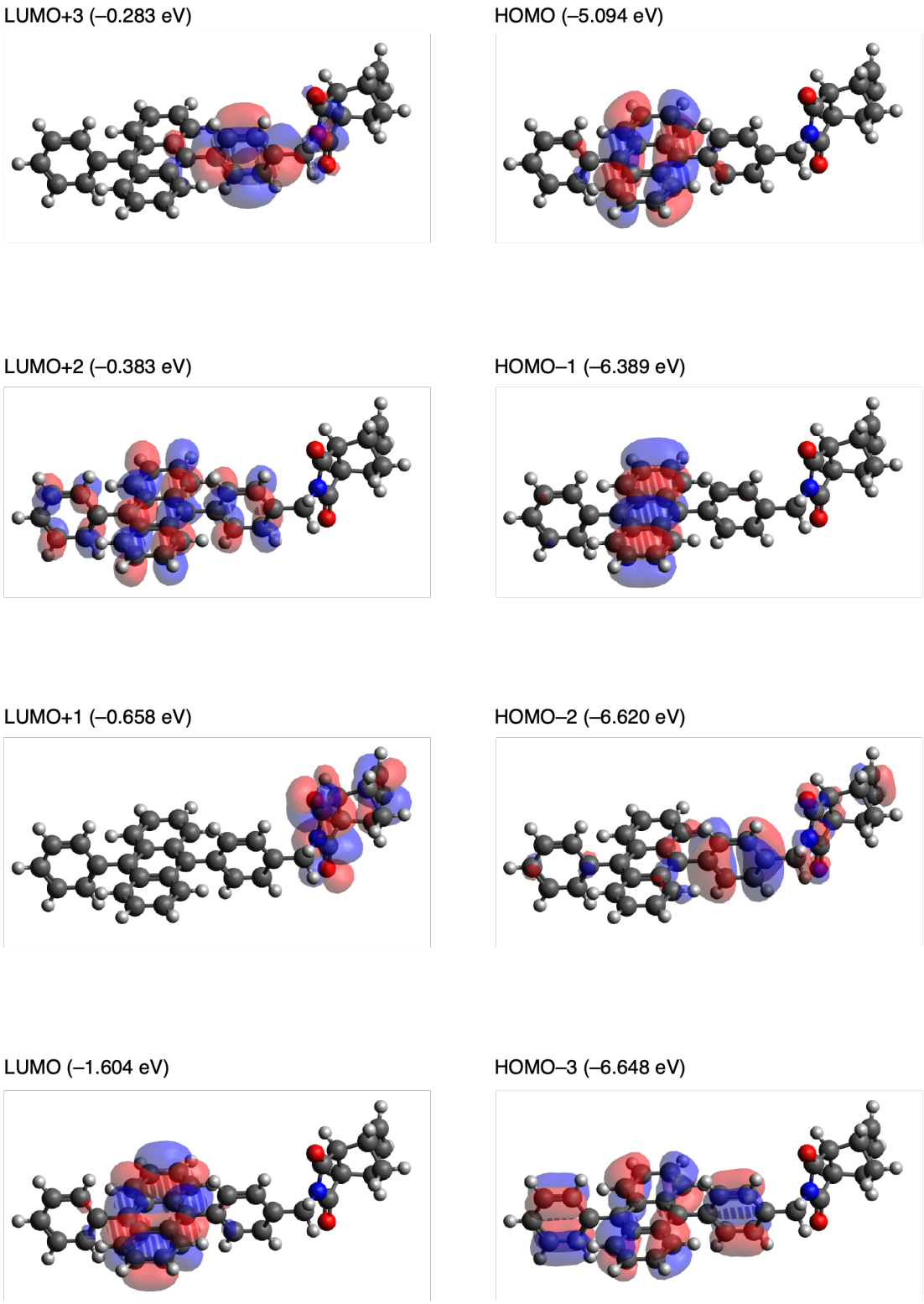

Fig. S41 Shapes and energy levels from LUMO+3 to HOMO–3 of **2** at the ground state obtained by the TD-DFT calculation (B3LYP/6-31G*, nstates = 40), corresponding to UV–vis absorption.

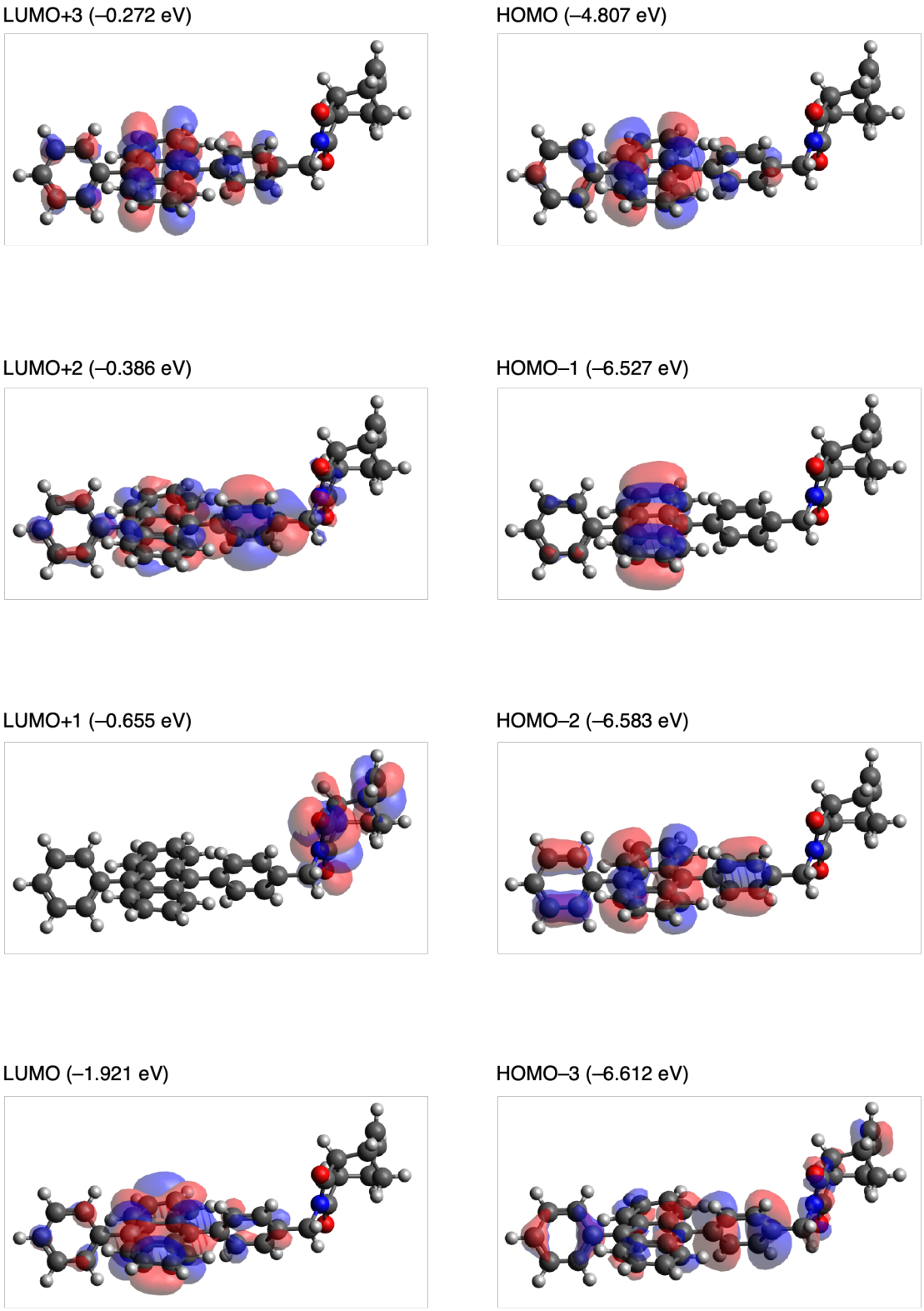

Fig. S42 Shapes and energy levels from LUMO+3 to HOMO–3 of **2** at the excited singlet state obtained by the TD-DFT calculation (B3LYP/6-31G*, nstates = 40), corresponding to fluorescence emission.

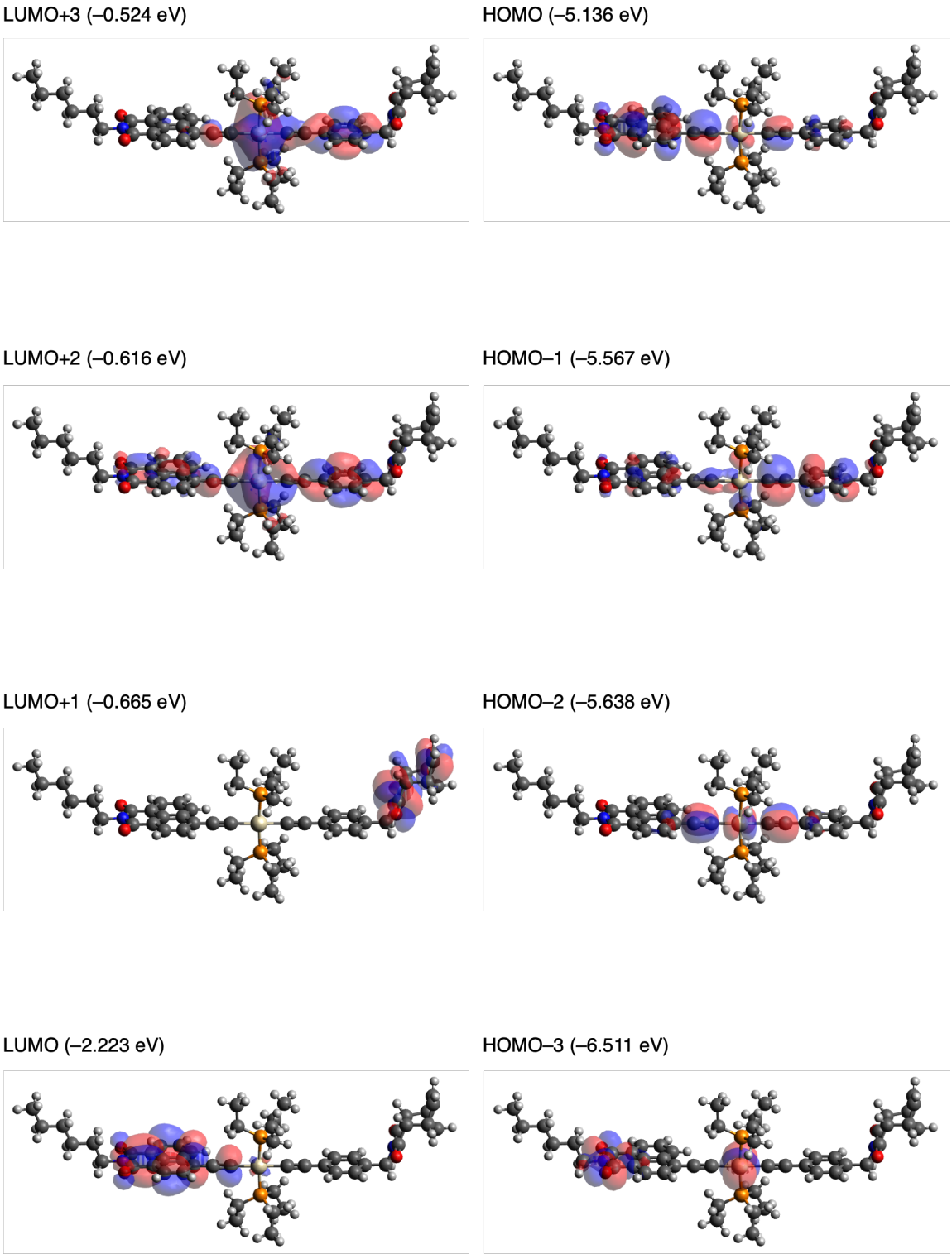

Fig. S43 Shapes and energy levels from LUMO+3 to HOMO–3 of **2** at the excited triplet state obtained by the TD-DFT calculation (B3LYP/6-31G*, nstates = 40), corresponding to phosphorescence emission.

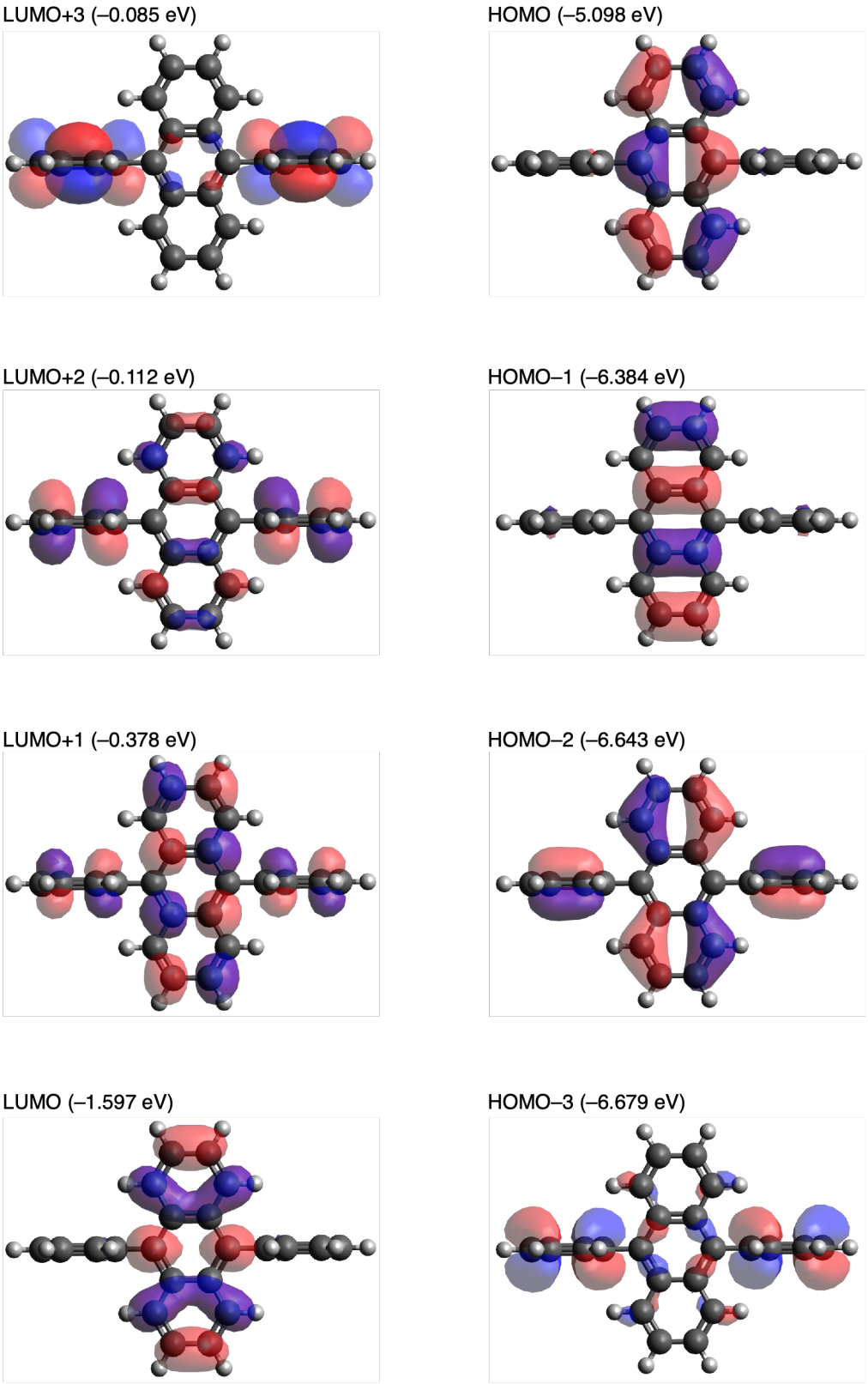

Fig. S44 Shapes and energy levels from LUMO+3 to HOMO–3 of DPA at the ground state obtained by the DFT calculation (B3LYP/6-31G*).

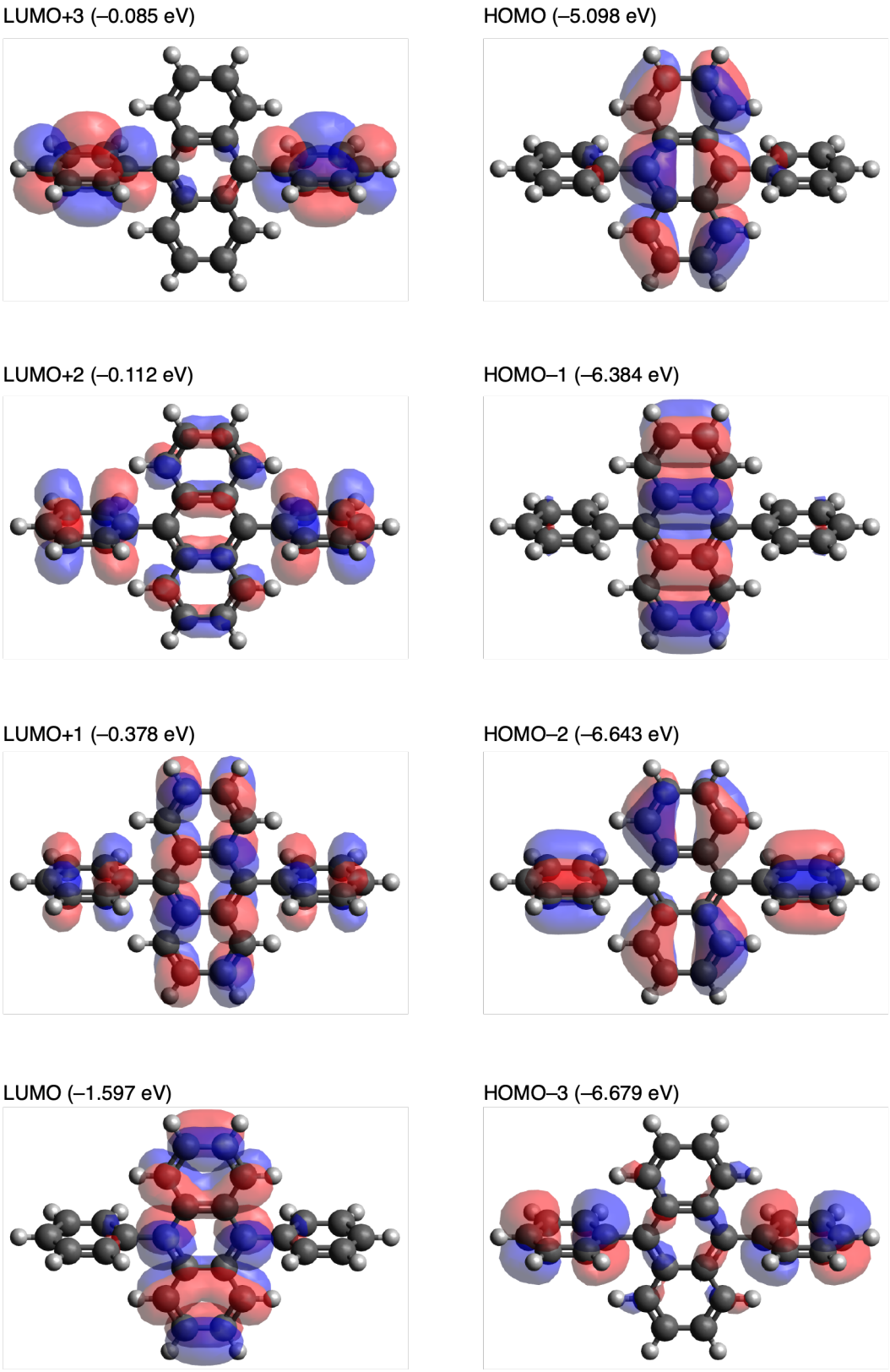

Fig. S45 Shapes and energy levels from LUMO+3 to HOMO–3 of DPA at the ground state obtained by the TD-DFT calculation (B3LYP/6-31G*, nstates = 40), corresponding to UV–vis absorption.

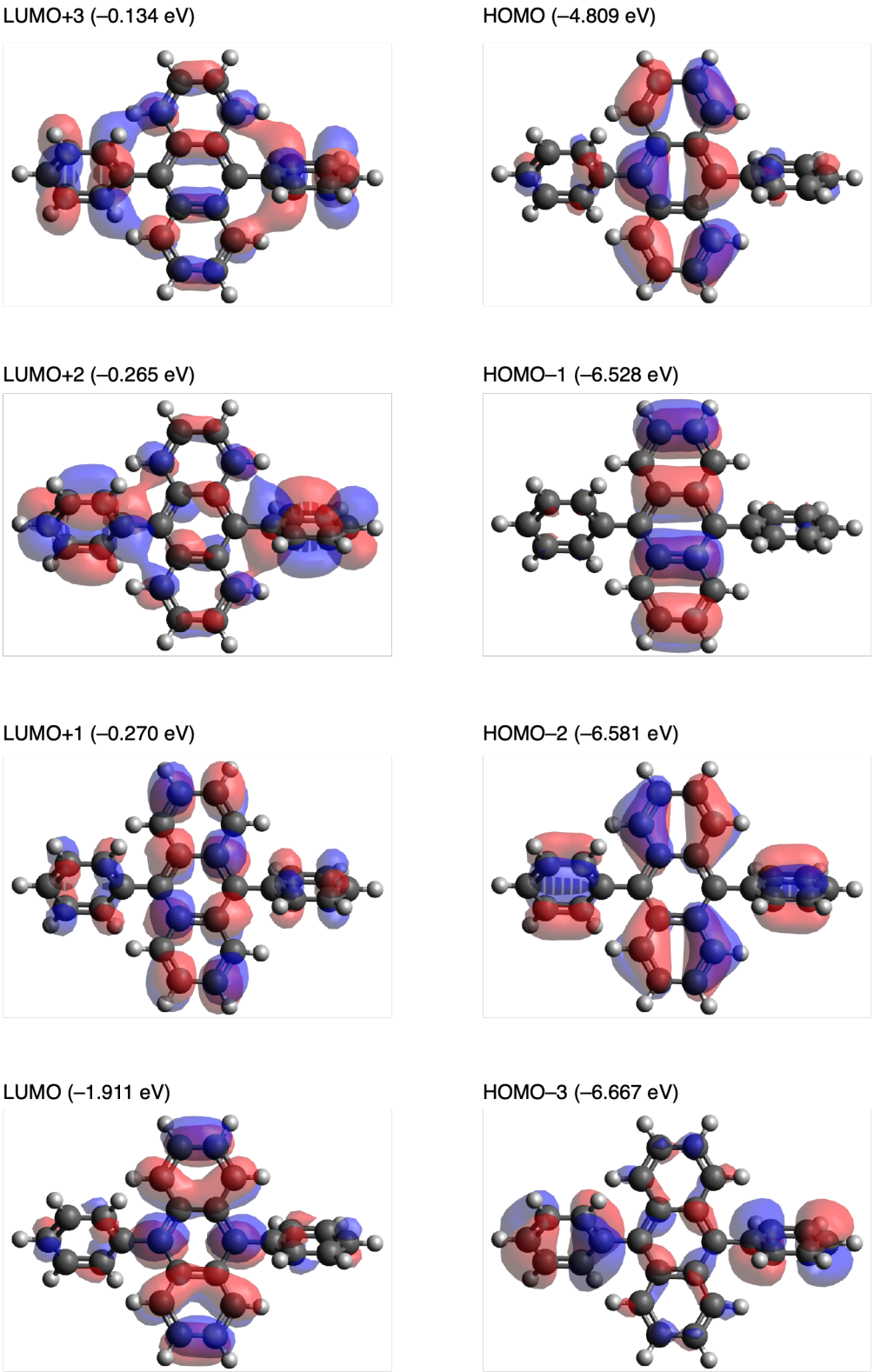

Fig. S46 Shapes and energy levels from LUMO+3 to HOMO–3 of DPA at the excited singlet state obtained the by TD-DFT calculation (B3LYP/6-31G*, nstates = 40), corresponding to fluorescence emission.

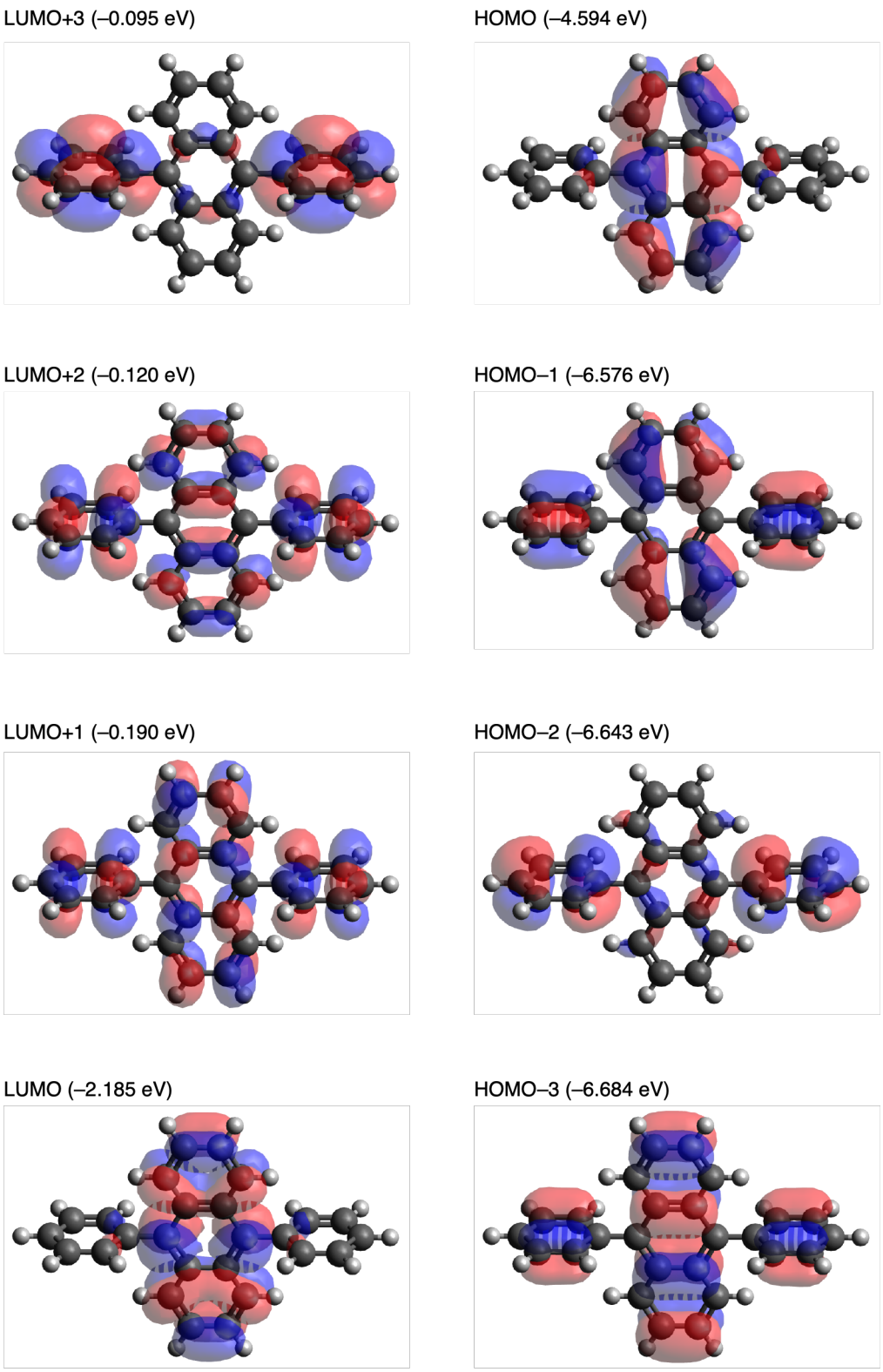

Fig. S47 Shapes and energy levels from LUMO+3 to HOMO–3 of DPA at the excited triplet state obtained by the TD-DFT calculation (B3LYP/6-31G*, nstates = 40), corresponding to phosphorescence emission.

References

S1) A. Naghipour, A. Ghorbani-Choghamarani, H. Babaee, M. Hashemi and B. Notash, Crystal structure of a novel polymorph of trans-dichlorobis(triphenylphosphine)palladium(II) and its application as a novel, efficient and retrievable catalyst for the amination of aryl halides and Stille cross-coupling reactions. *J. Organomet. Chem.*, 2017, **841**, 31–38.

S2) M. Ioele, G. Ortaggi, M. Scarsella and G. Sleiter, A rapid and convenient synthesis of tetrakis(triphenylphosphine)palladium(0) and -platinum(0) complexes by phase-transfer catalysis. *Polyhedron*, 1991, **10**, 2475–2476.

S3) K. O. Ali, H. A. Mohammad, T. Gerber and E. Hosten, Mixed Ligand, Palladium(II) and Platinum(II) Complexes of Tertiary Diphosphines with S-1H Benzo[D]Imidazole-2-Yl Benzothioate. *Orient. J. Chem.*, 2017, **33**, 584–592.

S4) S. Mukherjee, H. Dinda, L. Shashank, I. Chakraborty, R. Bhattacharyya, J. das Sarma, and R. Shunmugam, Site-specific amphiphilic magnetic copolymer nanoaggregates for dual imaging. *Macromolecules*, 2015, **48**, 6791–6800.

S5) F. Šembera, J. Plutnar, A. Higelin, Z. Janoušek, I. Císařová and J. Michl, Metal Complexes with Very Large Dipole Moments: the Anionic Carborane Nitriles 12-$NC{-}CB_{11}X_{11}^{-}$ (X = H, F, CH_3) as Ligands on Pt(II) and Pd(II). *Inorg. Chem.*, 2016, **55**, 3797–3806.

S6) N. Chuard, K. Fujisawa, P. Morelli, J. Saarbach, N. Winssinger, P. Metrangolo, G. Resnati, N. Sakai and S.Matile, Activation of Cell-Penetrating Peptides with Ionpair-π Interactions and Fluorophiles. *J. Am. Chem. Soc.*, 2016, **138**, 11264–11271.

S6) C. He, H. Guo, Q. Peng,; S. Dong and F. Li, Asymmetrically twisted anthracene derivatives as highly efficient deep-blue emitters for organic light-emitting diodes. *J. Mater. Chem. C*, 2015, **3**, 9942–9947.

S7) M. J. Frisch, G. W. Trucks, H. B. Schlegel, G. E. Scuseria, M. A. Robb, J. R. Cheeseman, G. Scalmani, V. Barone, G. A. Petersson, H. Nakatsuji, X. Li, M. Caricato, A. V. Marenich, J. Bloino, B. G. Janesko, R. Gomperts, B. Mennucci, H. P. Hratchian, J. V. Ortiz, A. F. Izmaylov, J. L. Sonnenberg, D. Williams-Young, F. Ding, F. Lipparini, F. Egidi, J. Goings, B. Peng, A. Petrone, T. Henderson, D. Ranasinghe, V. G. Zakrzewski, J. Gao, N. Rega, G. Zheng, W. Liang, M. Hada, M. Ehara, K. Toyota, R. Fukuda, J. Hasegawa, M. Ishida, T. Nakajima, Y. Honda, O. Kitao, H. Nakai, T. Vreven, K. Throssell, J. A. Montgomery, Jr., J. E. Peralta, F. Ogliaro, M. J. Bearpark, J. J. Heyd, E. N. Brothers, K. N. Kudin, V. N. Staroverov, T. A. Keith, R. Kobayashi, J. Normand, K. Raghavachari, A. P. Rendell, J. C. Burant, S. S. Iyengar, J. Tomasi, M. Cossi, J. M. Millam, M. Klene, C. Adamo, R. Cammi, J. W. Ochterski, R. L. Martin, K. Morokuma, O. Farkas, J. B. Foresman and D. J. Fox, Gaussian, Inc., Wallingford CT, 2016.

S8) Y. Zhou, F. N. Castellano, T. W. Schmidt and K. Hanson, On the Quantum Yield of Photon

Upconversion via Triplet−Triplet Annihilation. *ACS Energy Lett.*, 2020, **5**, 2322–2326.